High-Rydberg Dynamics: Intra- and Intermolecular

- Non-adiabatic coupling between excited electronic and internuclear degrees of freedom *challenges our understanding of chemical reactivity*.
- Electrons in transport interact with their surroundings *with consequences from solar energy conversion to cell biology*.
- Molecular Rydberg systems provide a useful laboratory for isolating and studying non-adiabatic electron-molecule interactions.

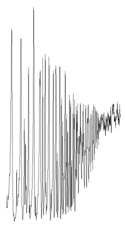

- Some things we can learn from spectroscopy about the forces that drive the relaxation of high-Rydberg states and systems.

1. Transient high-Rydberg states of BH: Dynamics of the coupling of orbital electronic with core rovibrational degrees of freedom

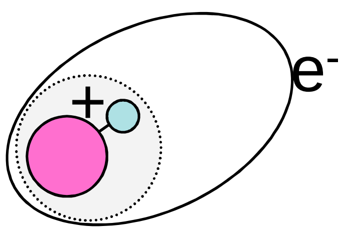

2. Collective relaxation in a cold gas of NO Rydbergs

Outline

- Rovibronic coupling in the high-Rydberg states of BH
  - A scattering formalism
  - Gateway state: 3sσ B $^1\Sigma^+$ in double resonance
  - High Rydbergs
    - Exchange of orbital and rotational angular momentum
    - Hundreds of states coupled over thousands of cm^{-1}
    - A single matrix element and its variation
    - Ultrafast vibrational relaxation: Autoionization
    - Neutral dissociation: Dissociative Recombination

NSERC
CRSNG

Ricardo Viteri, Frauke Schröder, Scott Rixon
Jason Clark,Andy Gilkison, Aaron Harrison

Rydberg states of BH selected by double resonance

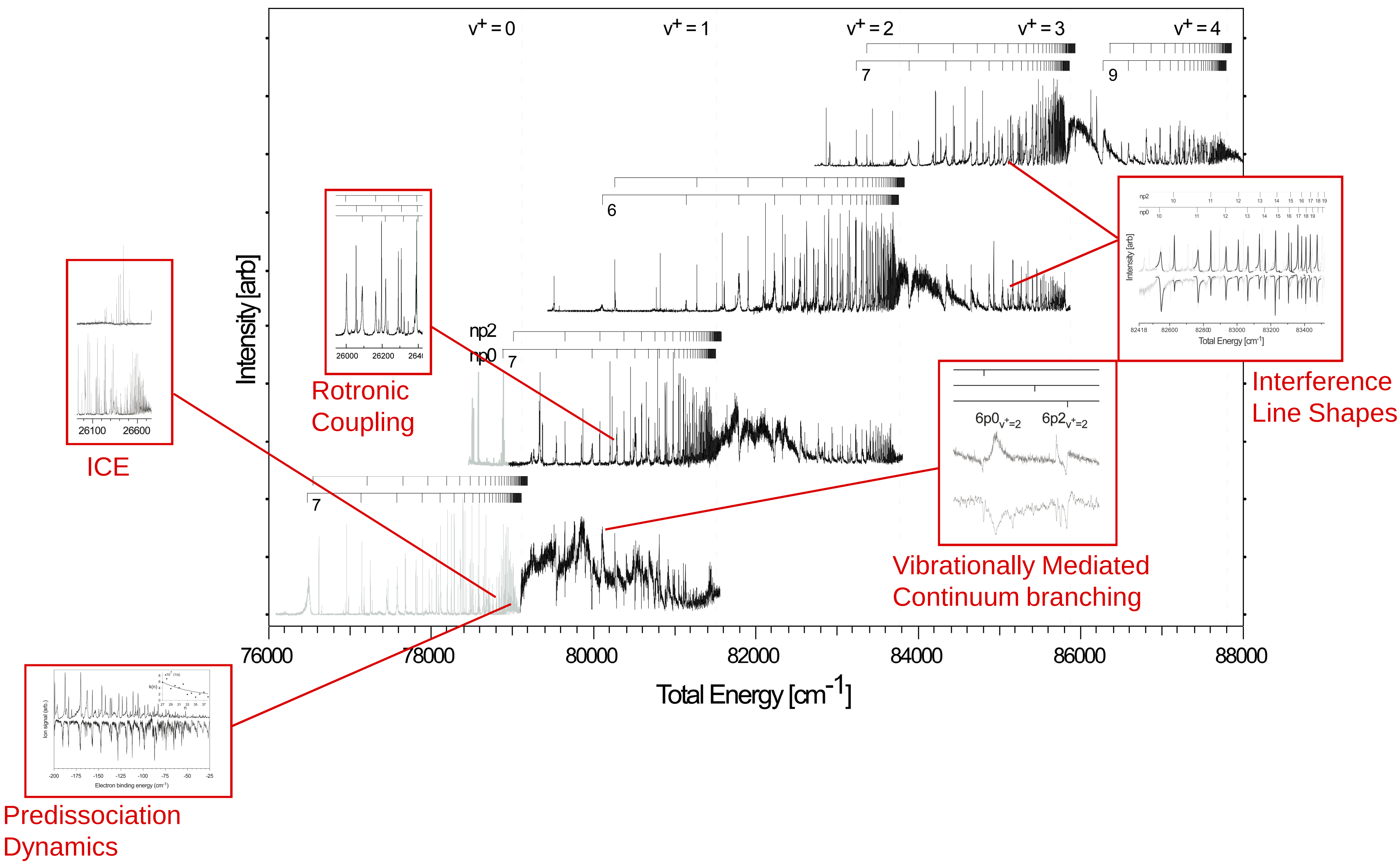

Cation-electron scattering in high-Rydberg states

At long range, a Rydberg electron sees the core as a charged sphere

- Core motions averaged
- Single-electron boundary conditions (H·, $E_i = I_i - Ryd / \nu_i^2$)
- Complex systems of states, sensitive to total energy

Close to the core, the electron joins many-body interactions with other electrons and nuclei

- Electrons matter, and interaction depends on orbital angular momentum (penetration varies, *s,p,d, f*, like atoms)
- Internuclear axis matters, and interaction depends on orbital orientation ($\lambda = \sigma, \pi, \delta, \ldots$)
- Internuclear distance matters, and interaction depends on turning point

Cation-electron scattering in high-Rydberg states

At long range, a Rydberg electron sees the core as a charged sphere

- Core motions averaged
- Single-electron boundary conditions (H•, $E_i = I_i - Ryd / \nu_i^2$)
- Complex systems of states, sensitive to total energy

Close to the core, the electron joins many-body interactions with other electrons and nuclei

- Electrons matter, and interaction depends on *l*
- Internuclear axis matters, and interaction depends λ
- Internuclear distance matters, and interaction depends r

- Coupling occurs here
- Scattering dynamics independent of asymptotic energy
- Electron strobes internuclear distance
- Rapid passage of electron projects the inner eigenstates on the outer ones (frame transformation)

Coulomb attraction at long range yields states in series defined by effective principal quantum numbers, ν_i

$$E_i = I_i - \frac{Ryd}{\nu_i^2} \qquad\qquad \nu_i = n - \delta_i$$

where ν_i determined by long range boundary conditions that limit wavefunctions to those for which coefficients satisfy

$$\det\left|\delta_{ij}\tan\pi\nu_i + R_{ij}\right| = 0$$

For a single channel, and $R_{11} = 0$, this gives the H atom ($\delta_1 = 0$ and $\nu = 1, 2, 3\ldots$)

For many-electron atoms and molecules, R_{ij} allows for a finite core and multichannel interactions

For two channels, say 0 and 2, we can write explicitly:

$$\begin{vmatrix} \tan\pi(\nu_0+\mu_0) & \xi \\ \xi & \tan\pi(\nu_2+\mu_2) \end{vmatrix} = \tan\pi(\mu_0-\delta_0)\tan\pi(\mu_2-\delta_2) - \xi^2 = 0$$

where we write R_{00} as μ_0, etc. $\nu_0 = n - \delta_0$

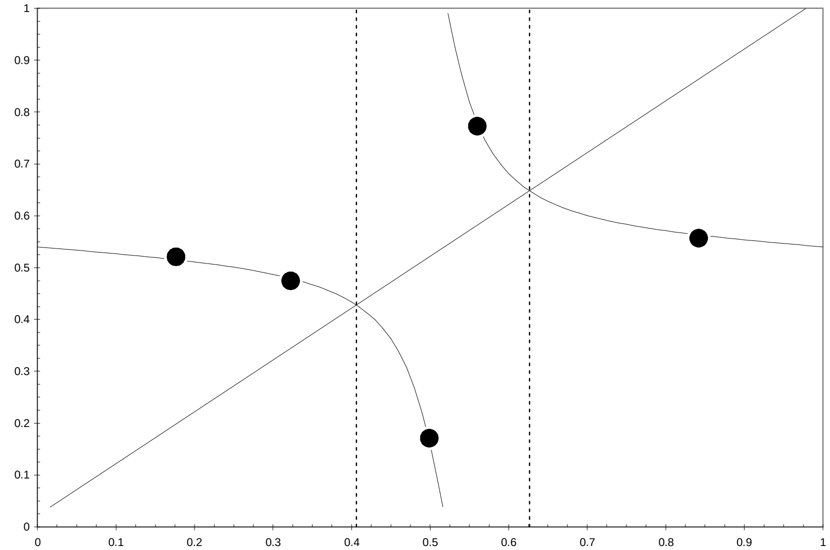

δ_2 δ_0

Lu – Fano plot

Visible followed by UV excitation selects a single rovibrational level (v', $N' = 0$) of the gateway 3s ʃ B $^1\Sigma^+$ Rydberg state in ^{11}BH

Subsequent excitation yields ions, via vibrational autoionization or by predissociation followed by UV photoionization of excited boron atoms.

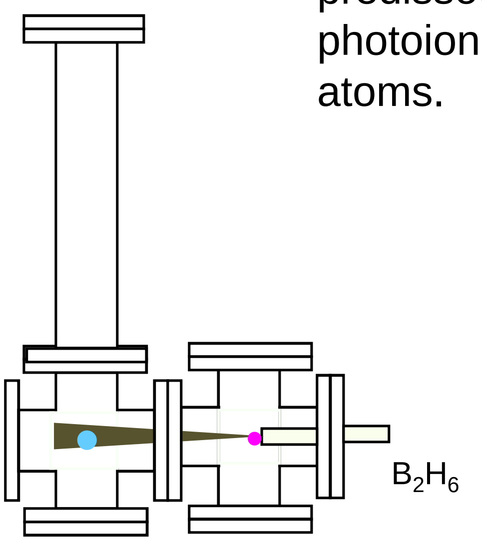

ω_1, ω_2, ω_3 193 mn

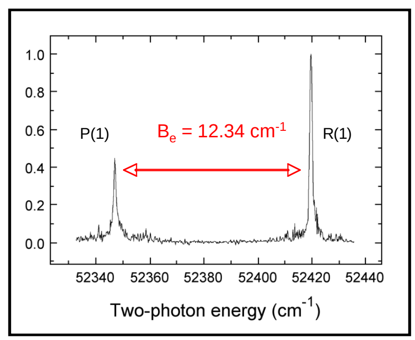

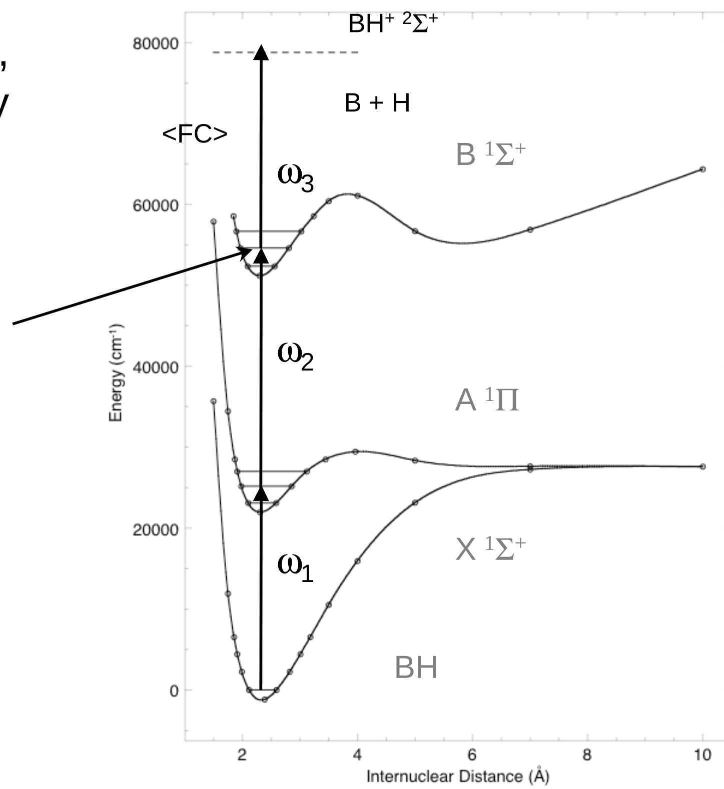

Selection rules allow only final angular momentum $N = 1$

Optical selection isolates single rovibronic lines all with *N = 1*

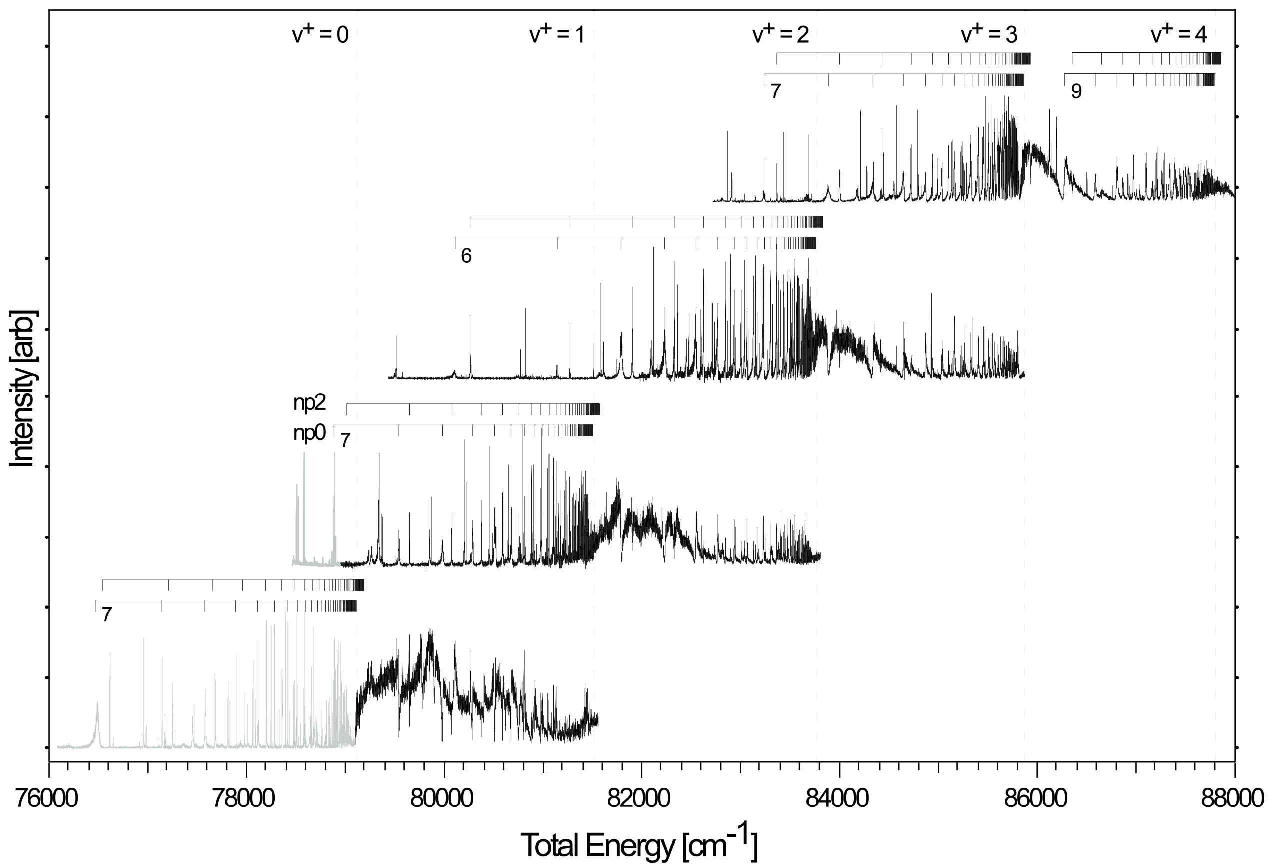

ns(N^+=1), np(N^+=0), np(N^+=2), nf(N^+=2)

$+ \rightarrow -$ parity selection rules allow transitions from B $^1\Sigma^+$ N' = 0 to rotational levels that form series converging to BH^+ $N^+ = 0$, 1 and 2

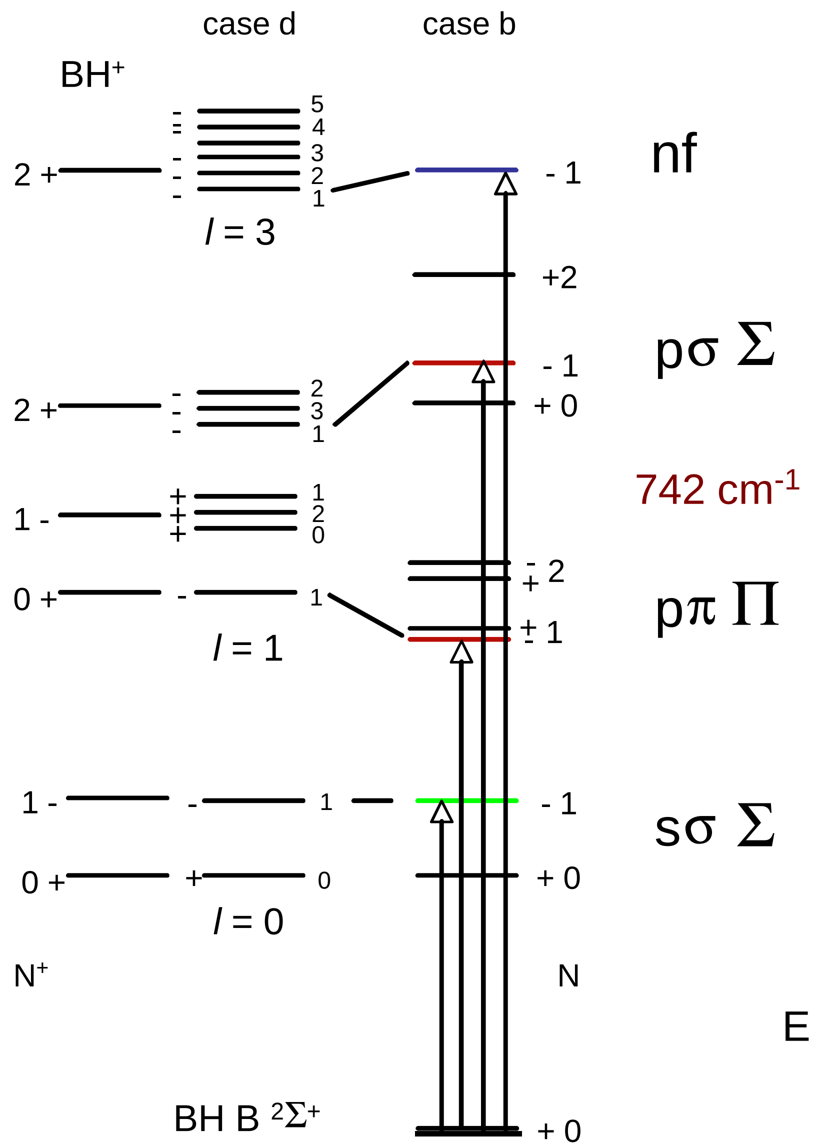

n= 3

$\mu_2 = 0.4791$

$\mu_0 = 0.5316$

$\mu_1 = 0.975$

$$E = IP_{N^+} - \frac{Ryd}{(n - \mu_{N^+})^2}$$

Resonances assigned to rotational limits plotted as a function of observed quantum defect

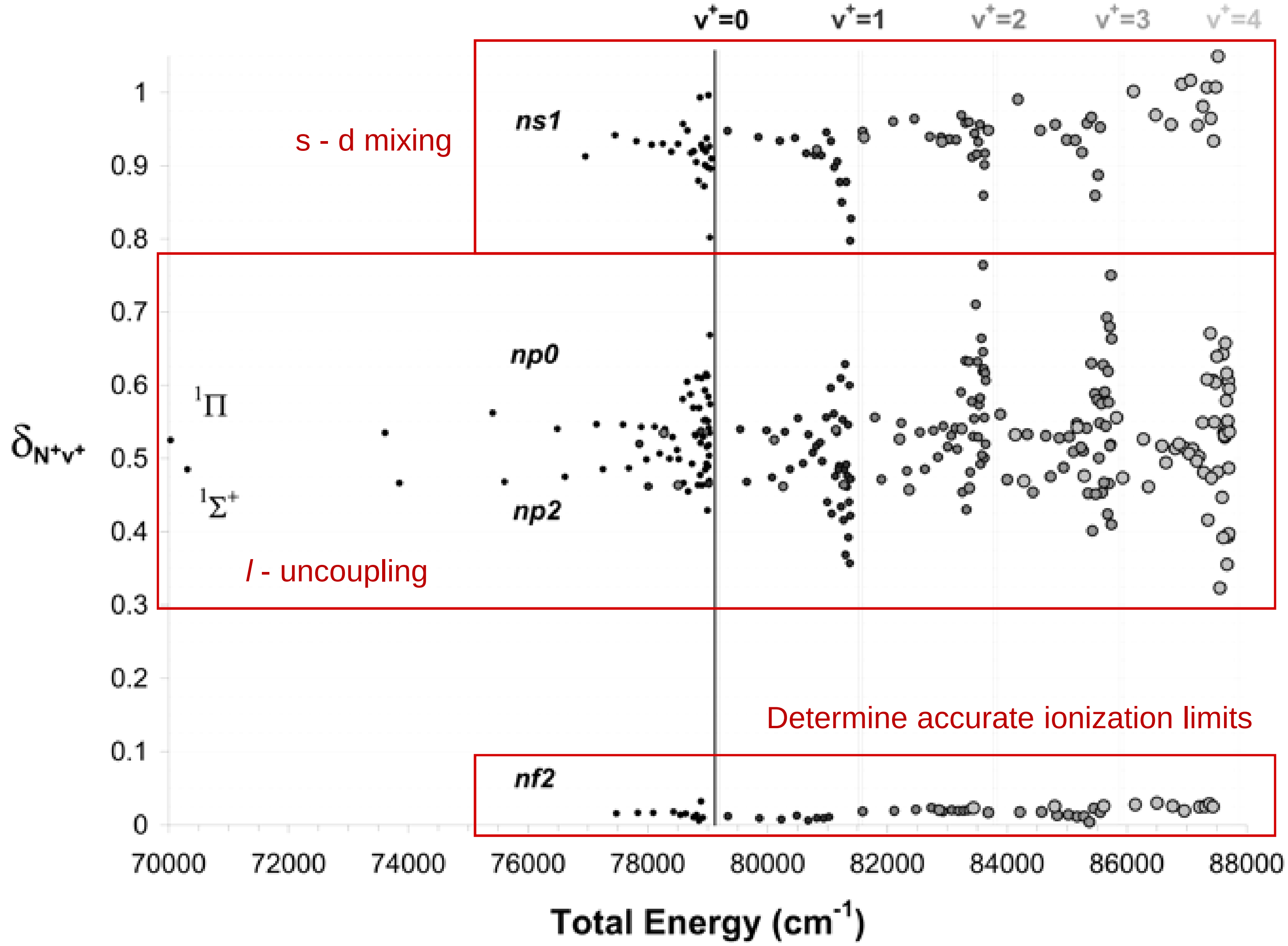

Lu-Fano plot compactly represents the coupling of electronic orbital and rotational angular momentum over the complete energy interval

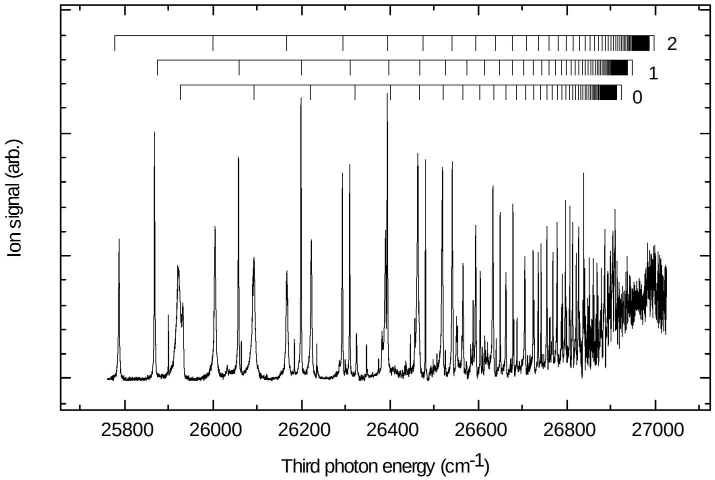

$$\tan\pi(\mu_0-\delta_0)\tan\pi(\mu_2-\delta_2)-\xi^2=0$$

$$\xi=0.36$$

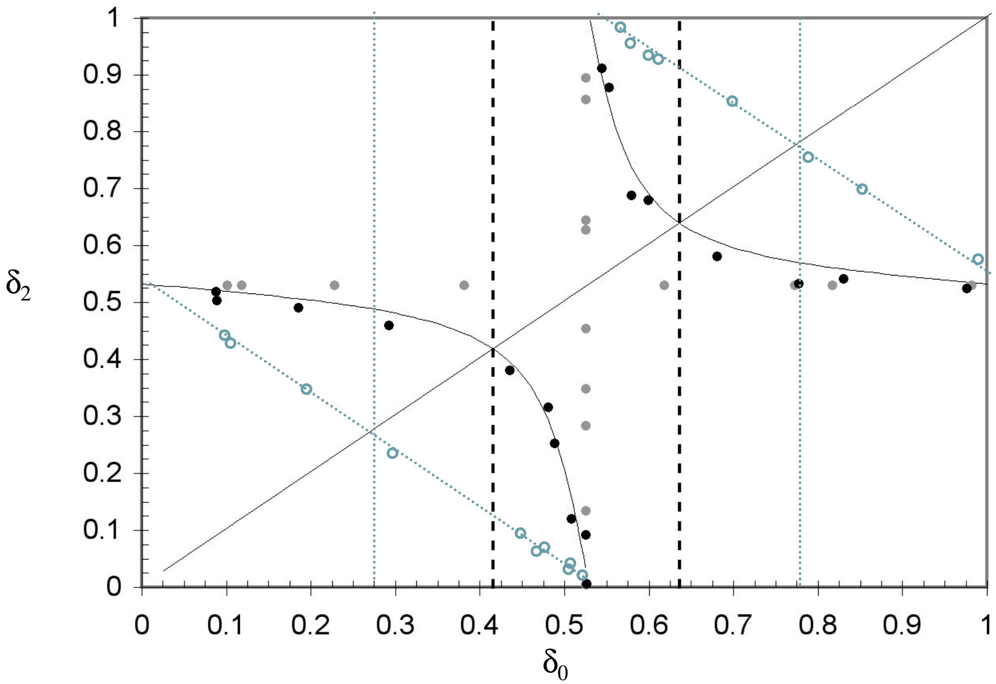

points at which:

$\tan\pi(\mu_0-\delta_0)=\tan\pi(\mu_2-\delta_2)=\pm\xi$

mark the avoided crossing

Define an index:

$$\xi=\tan\pi\eta$$

$$\eta=0.11$$

For η =0.25, parallel lines of slope 1, complete mixing

Lu – Fano avoided crossings characterize the strength of rotational channel coupling between the *np(N⁺=0 and 2)* channels

$$\tan\pi\left(\mu_0-\delta_0\right)\tan\pi\left(\mu_2-\delta_2\right)-\xi^2=0$$

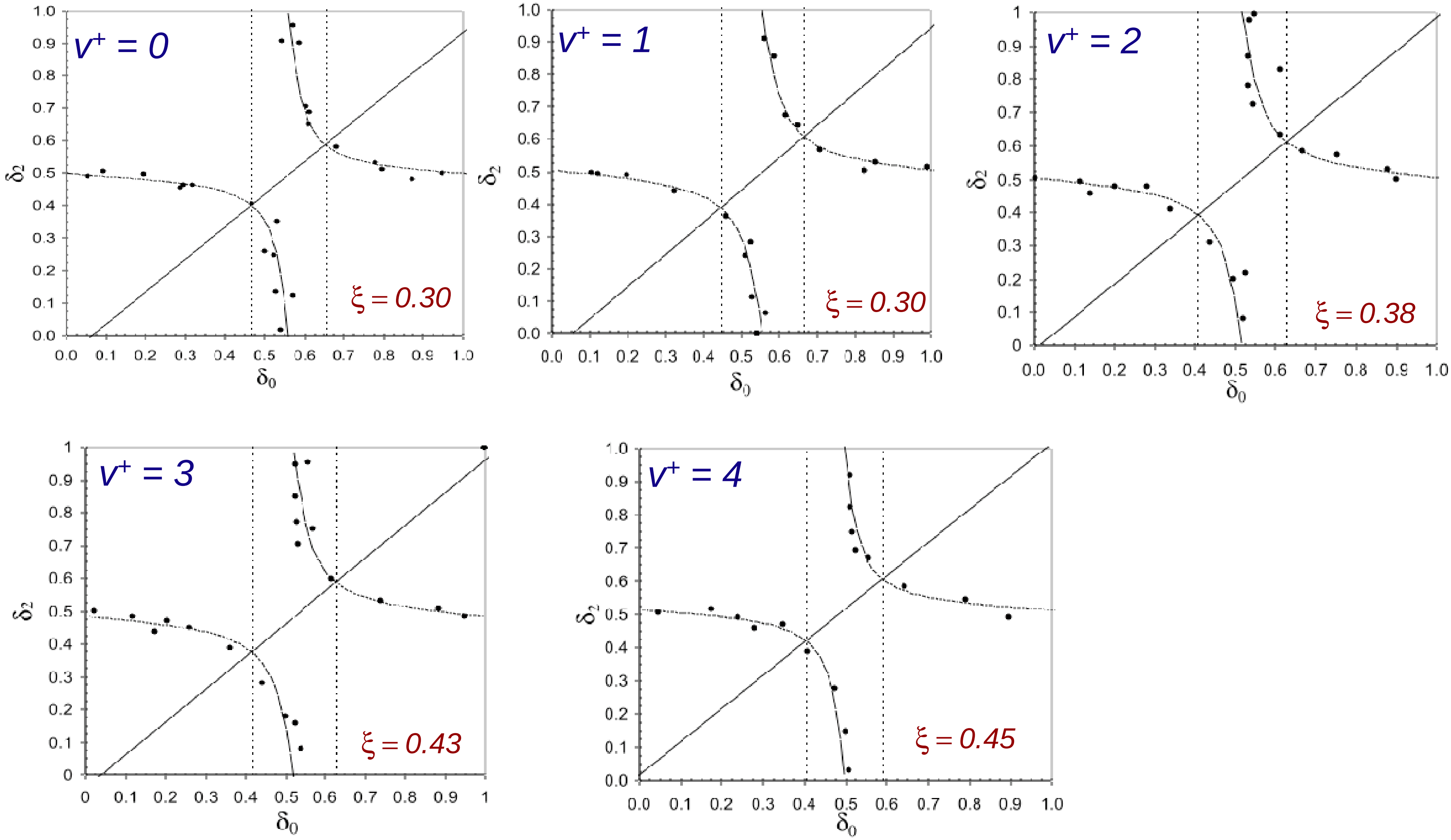

Eigenchannel quantum defects accounting for l-uncoupling at low n as a function of v

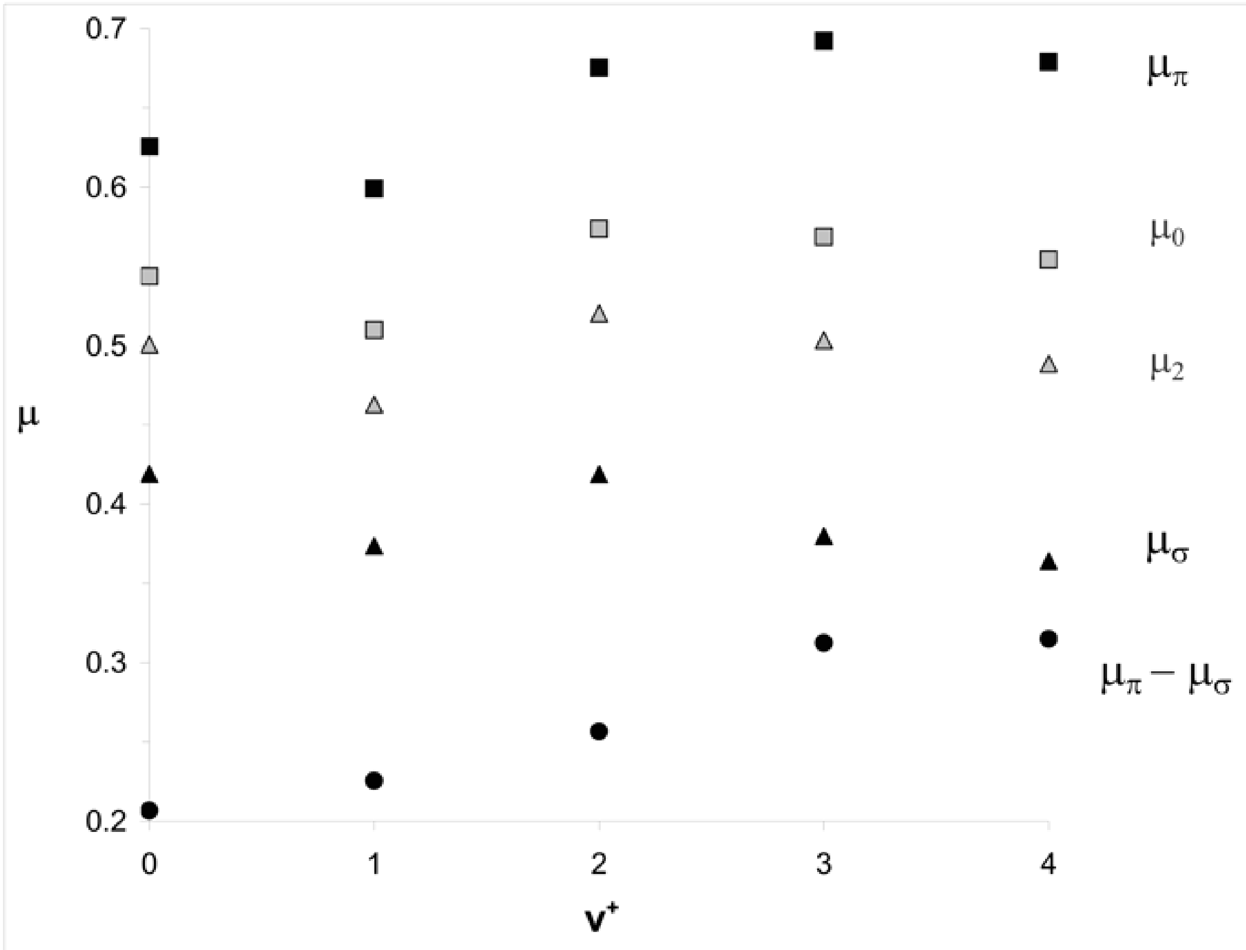

BH resonances observed in ω_3 transitions from B $^1\Sigma^+$ v' = 0, N' = 0

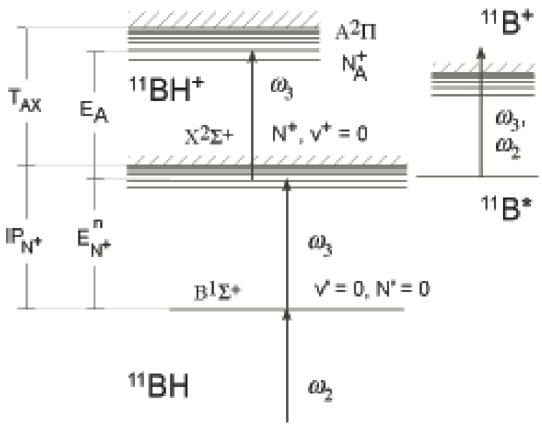

Detect absorption below the $v^+ = 0$ limit as B^+ action spectrum

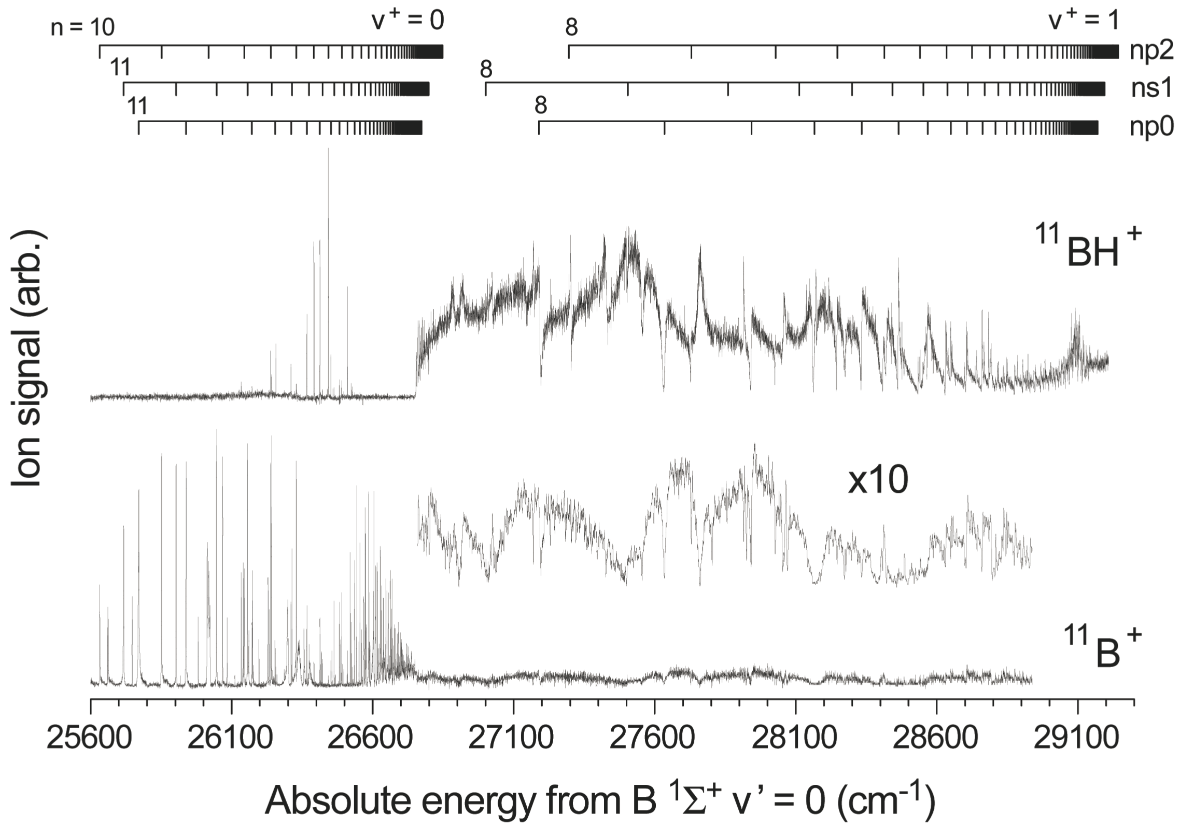

ICE gauges the rate of photoexcitation in competition with predisociation

$$\frac{[^{11}BH^{*}|A^{2}\Pi\rangle|nl\rangle]}{[^{11}B^{*}]} = \frac{I_{12}^{n}}{I_{11}^{n}/\left(1-\mathrm{e}^{-k(n)\cdot 10\mathrm{ns}}\right)} = \frac{\Phi\cdot\sigma_{AX}}{k(n)}$$

Yield ratio ($ʃ_{AX}$ *determined by* $\wp_{A}$ *and detuning)*

$$I_{N+}^{n}(\omega_3) = \left[I_{11}^{n}/\left(1-\mathrm{e}^{-k(n)\cdot 10\mathrm{ns}}\right) + I_{12}^{n}\right]\cdot\left[1+\left(\frac{\omega_3 - E_{N+}^{n}}{\Gamma_{X}^{n}}\right)^{2}\right]^{-1}$$

Lorentzian lineshape

$$I_{12}^{sim}(\omega_3) = \sum_{n,N^+} I_{N+}^{n}(\omega_3)\cdot\left[\frac{k(n)}{\Phi(\omega_3)\cdot\sigma_{AX}(n,N^+)}+1\right]^{-1}$$

Line proportion to BH^+

- Assume transitions conserve |*n,l*>
- Assume invariant quantum defect
- Use theoretical oscillator strength
- Estimate *k(n)* from the signal at high *n*
- Fit $\wp_{A}$

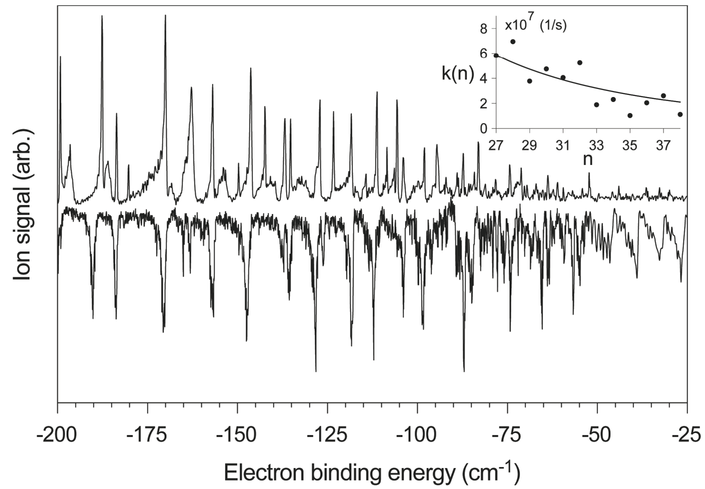

Predissociation lifetimes on the order of 1 ns, but linewidths comparable to those observed for autoionizing resonances

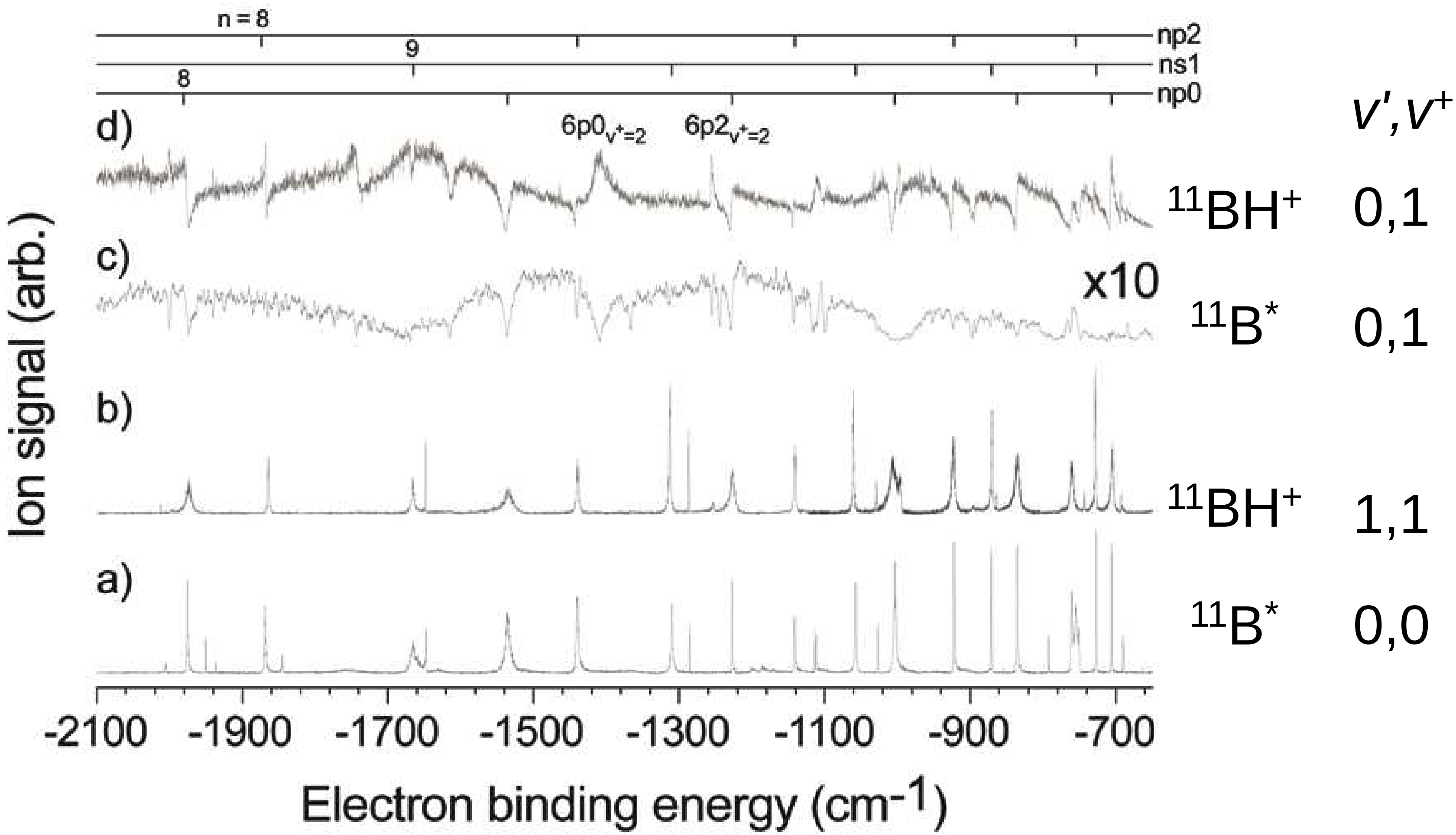

- Discrete states couple to a common continuum (see Jungen & Ross PRA 55 R2503)
- Increased amplitude in r_{BH} favors ionization

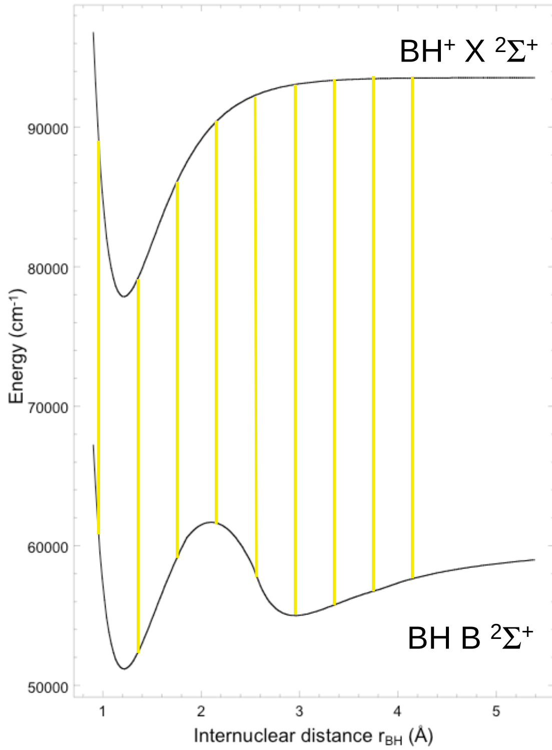

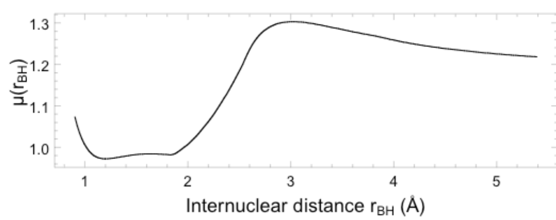

Electron-cation collisions much faster than vibration. Close-coupled binding energy as a function of bond distance determines $\mu(r_{BH})$.

$$E\left(r_{BH}\right) = \frac{Ryd}{\left(n-\mu\left(r_{BH}\right)\right)^2}$$

$\mu(r_{BH})$ determines the electronic phase shift for fixed r_{BH}.

Through its r_{BH}-dependence, $\mu(r_{BH})$ couples channel wavefunctions built on different vibrational states of the core (V_{ij}):

$$\left\langle \psi_{l+D}\left(\omega_3\right)\chi_{v+-1}\middle| H \middle| nlN^+\chi_{v+}\right\rangle = \frac{d\mu^{\Lambda}\left(r_{BH}\right)}{dr_{BH}}\left[\frac{h}{8\pi^2 c\omega}\right]\sqrt{v^+}$$

Also determines FC factors.

Rydberg series converging to BH^+ $v^+ = 1$ observed in vertical transitions from B $^1\Sigma^+$ $N' = 0$, $v' = 1$ compared with $\Delta v = v' + 1$ transitions from $v' = 0$

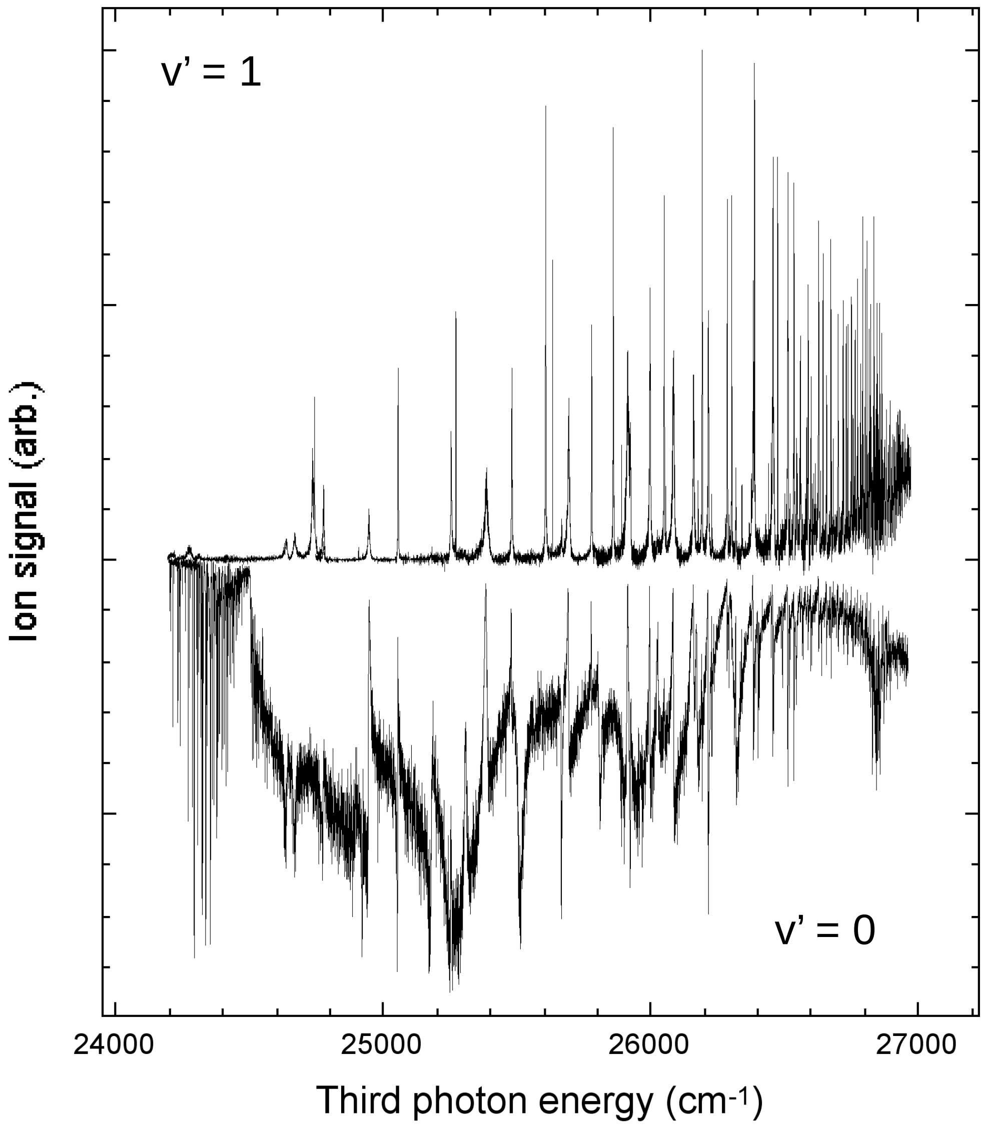

$$\sigma(\varepsilon) = \frac{(q+\varepsilon)^2}{(1+\varepsilon^2)} \qquad \varepsilon = \frac{(E - E_R)}{\Gamma/2}$$

$$q = \frac{\langle np\lambda | T | 3s\sigma \rangle \langle \chi_{v=i} | \chi'_{v=i} \rangle}{\langle \Psi_{I+D} | T | 3s\sigma \rangle \langle \chi_{v=i-1} | \chi'_{v=i} \rangle \pi V_{i-1,i}}$$

$$q = \frac{\langle np\lambda | T | 3s\sigma \rangle \langle \chi_{v=i+1} | \chi'_{v=i} \rangle}{\langle \Psi_{I+D} | T | 3s\sigma \rangle \langle \chi_{v=i} | \chi'_{v=i} \rangle \pi V_{i,i+1}}$$

Rydberg series converging to BH^+ $v^+ = 2$ observed in vertical transitions from B $^1\Sigma^+$ $N' = 0$, $v' = 2$ compared with $\Delta v = v' + 1$ transitions from $v' = 1$

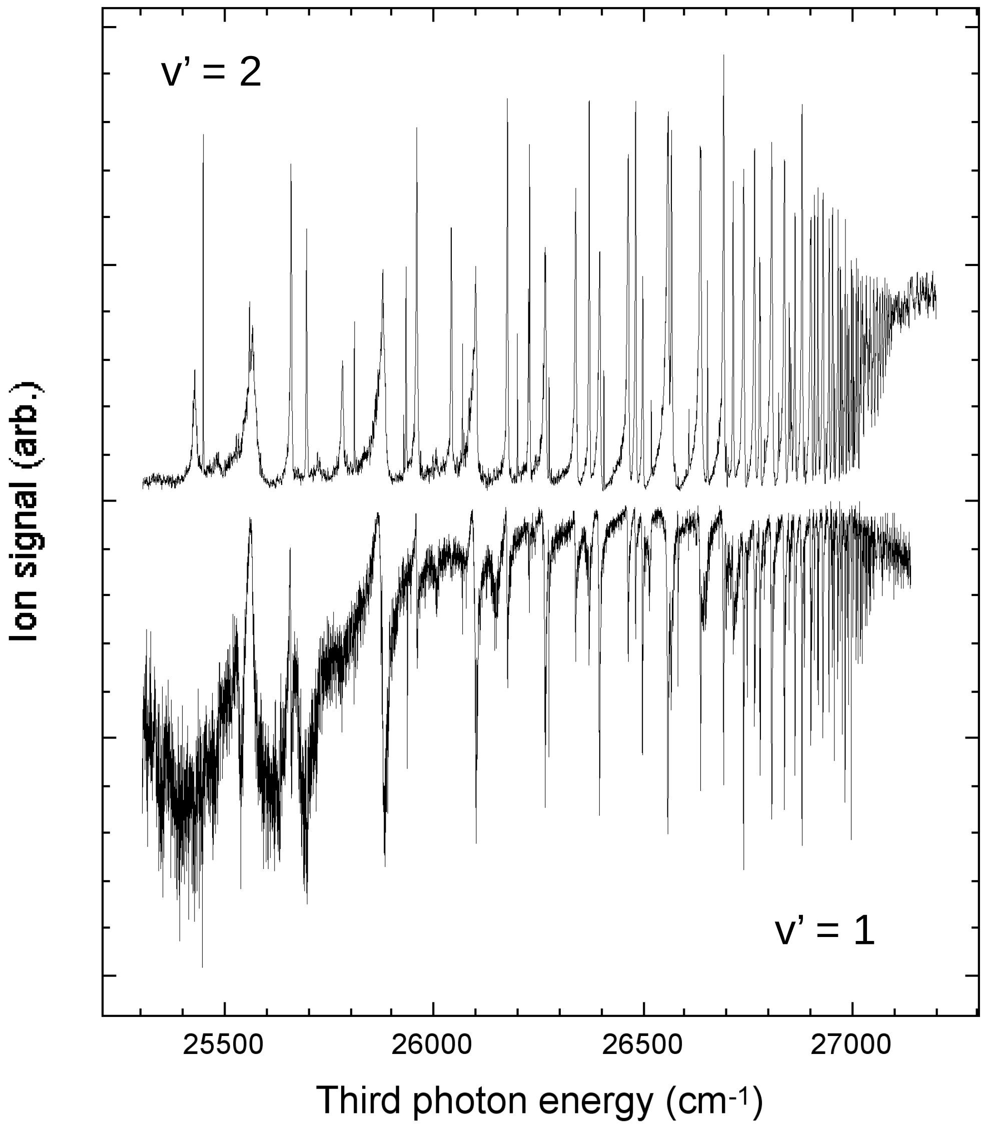

$$\sigma(\varepsilon) = \frac{(q+\varepsilon)^2}{(1+\varepsilon^2)} \qquad \varepsilon = \frac{(E - E_R)}{\Gamma/2}$$

$$q = \frac{\langle np\lambda | T | 3s\sigma \rangle \langle \chi_{v=i} | \chi'_{v=i} \rangle}{\langle \Psi_{I+D} | T | 3s\sigma \rangle \langle \chi_{v=i-1} | \chi'_{v=i} \rangle \pi V_{i-1,i}}$$

$$q = \frac{\langle np\lambda | T | 3s\sigma \rangle \langle \chi_{v=i+1} | \chi'_{v=i} \rangle}{\langle \Psi_{I+D} | T | 3s\sigma \rangle \langle \chi_{v=i} | \chi'_{v=i} \rangle \pi V_{i,i+1}}$$

Rydberg series converging to BH^+ $v^+ = 3$ observed in vertical transitions from B $^1\Sigma^+$ N' = 0, v' = 3 compared with $\Delta v = v' + 1$ transitions from v' = 2

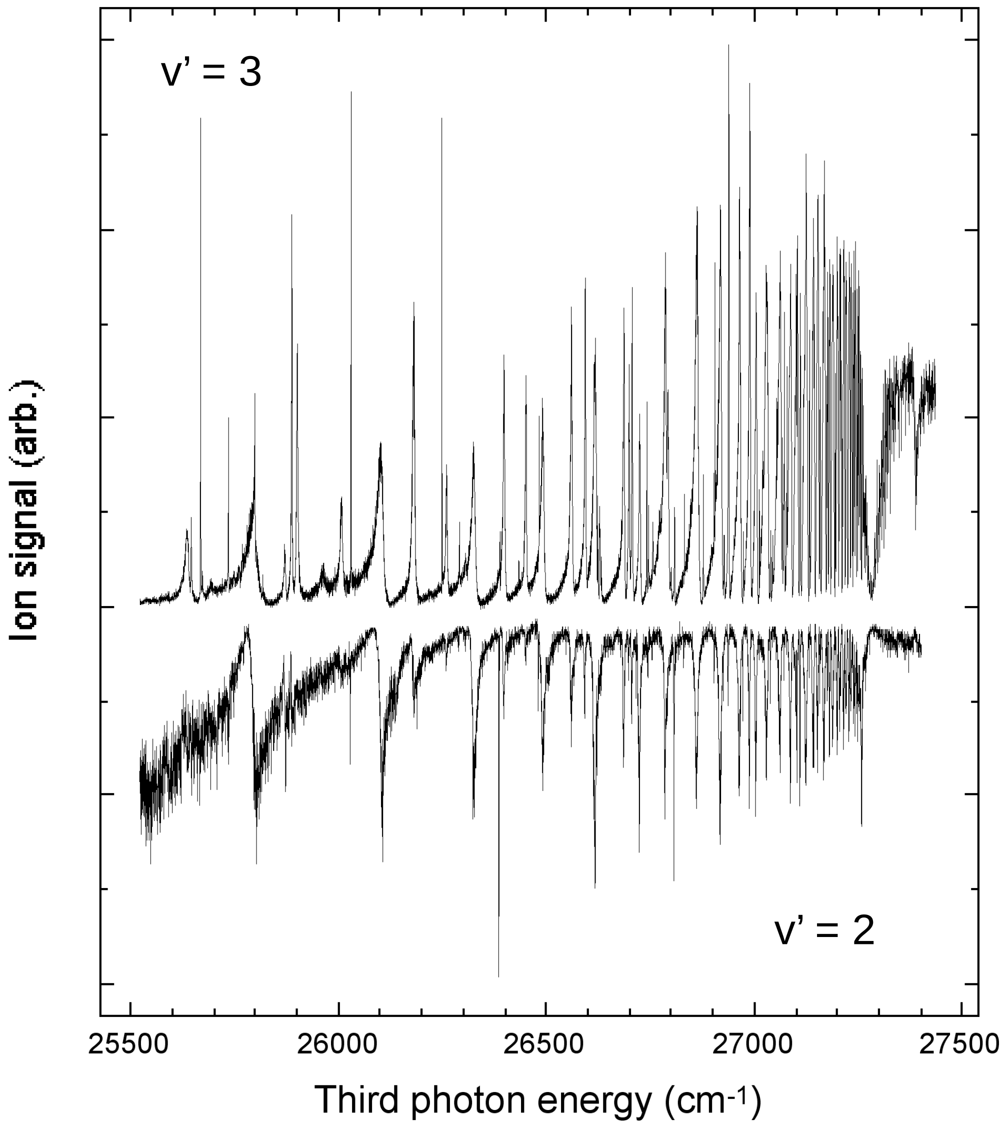

$$\sigma(\varepsilon) = \frac{(q+\varepsilon)^2}{(1+\varepsilon^2)} \qquad \varepsilon = \frac{(E - E_R)}{\Gamma/2}$$

$$q = \frac{\langle np\lambda | T | 3s\sigma \rangle \langle \chi_{v=i} | \chi'_{v=i} \rangle}{\langle \Psi_{I+D} | T | 3s\sigma \rangle \langle \chi_{v=i-1} | \chi'_{v=i} \rangle \pi V_{i-1,i}}$$

$$q = \frac{\langle np\lambda | T | 3s\sigma \rangle \langle \chi_{v=i+1} | \chi'_{v=i} \rangle}{\langle \Psi_{I+D} | T | 3s\sigma \rangle \langle \chi_{v=i} | \chi'_{v=i} \rangle \pi V_{i,i+1}}$$

Global trends in q explained by phases in vibrational overlap integrals

$$q=\frac{\left\langle np\lambda\right|T\left|3s\sigma\right\rangle\left\langle\chi_{v=3}\middle|\chi'_{v=3}\right\rangle}{\left\langle\Psi_{I+D}\right|T\left|3s\sigma\right\rangle\left\langle\chi_{v=2}\middle|\chi'_{v=3}\right\rangle\pi V_{23}}\quad q=\frac{\left\langle np\lambda\right|T\left|3s\sigma\right\rangle\left\langle\chi_{v=4}\middle|\chi'_{v=3}\right\rangle}{\left\langle\Psi_{I+D}\right|T\left|3s\sigma\right\rangle\left\langle\chi_{v=3}\middle|\chi'_{v=3}\right\rangle\pi V_{34}}$$

$$q=\frac{\left\langle np\lambda\right|T\left|3s\sigma\right\rangle\left\langle\chi_{v=2}\middle|\chi'_{v=2}\right\rangle}{\left\langle\Psi_{I+D}\right|T\left|3s\sigma\right\rangle\left\langle\chi_{v=1}\middle|\chi'_{v=2}\right\rangle\pi V_{12}}\quad q=\frac{\left\langle np\lambda\right|T\left|3s\sigma\right\rangle\left\langle\chi_{v=3}\middle|\chi'_{v=2}\right\rangle}{\left\langle\Psi_{I+D}\right|T\left|3s\sigma\right\rangle\left\langle\chi_{v=2}\middle|\chi'_{v=2}\right\rangle\pi V_{23}}$$

$$q=\frac{\left\langle np\lambda\right|T\left|3s\sigma\right\rangle\left\langle\chi_{v=1}\middle|\chi'_{v=1}\right\rangle}{\left\langle\Psi_{I+D}\right|T\left|3s\sigma\right\rangle\left\langle\chi_{v=0}\middle|\chi'_{v=1}\right\rangle\pi V_{01}}\quad q=\frac{\left\langle np\lambda\right|T\left|3s\sigma\right\rangle\left\langle\chi_{v=2}\middle|\chi'_{v=1}\right\rangle}{\left\langle\Psi_{I+D}\right|T\left|3s\sigma\right\rangle\left\langle\chi_{v=1}\middle|\chi'_{v=1}\right\rangle\pi V_{12}}$$

$$q=\frac{\left\langle np\lambda\right|T\left|3s\sigma\right\rangle\left\langle\chi_{v=0}\middle|\chi'_{v=0}\right\rangle}{\left\langle\Psi_{I'+D}\right|T\left|3s\sigma\right\rangle\left\langle\chi_{v=0}\middle|\chi'_{v=0}\right\rangle\pi V_{cont}}\quad q=\frac{\left\langle np\lambda\right|T\left|3s\sigma\right\rangle\left\langle\chi_{v=1}\middle|\chi'_{v=0}\right\rangle}{\left\langle\Psi_{I+D}\right|T\left|3s\sigma\right\rangle\left\langle\chi_{v=0}\middle|\chi'_{v=0}\right\rangle\pi V_{01}}$$

Trend in Γ (V_{v^+,v^+-1}) as a function of v^+

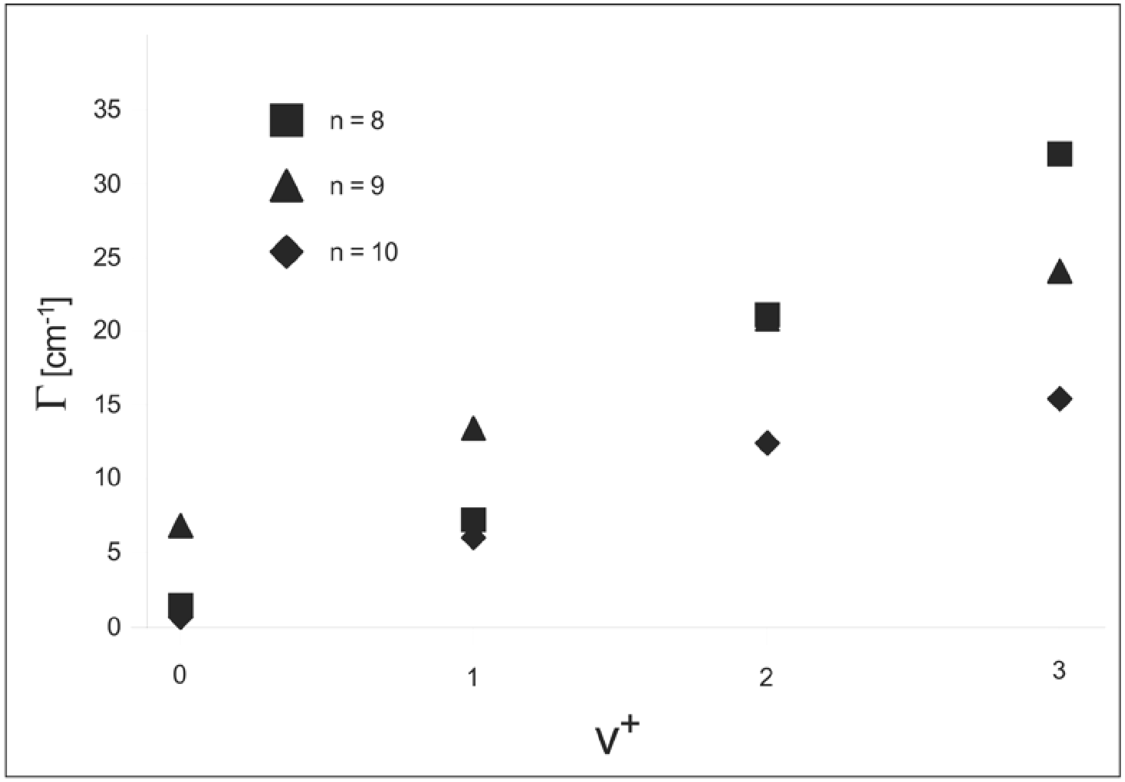

Conclusions

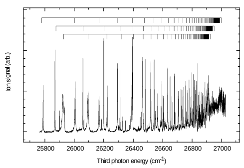

Triple resonance spectroscopy isolates high-Rydberg states of BH converging to $v^+ = 1 - 4$ for which $N = 1$.

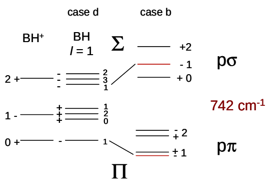

Coriolis (*l*-uncoupling) interaction mixes electron orbital angular momentum with core rotation

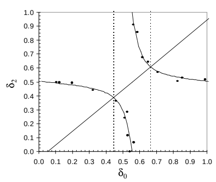

2000 cm^{-1} of perturbed structure characterized in terms of a single parameter by the Lu-Fano analysis of quantum defects

- Well-defined projection of orbital angular momentum on the internuclear axis gives way to *l*-uncoupling with increasing *n*
- Rotronic interaction appears as an *np* ($N^+ = 0,2$) avoided crossing at $n = 14$, characterized by $\xi = 0.30$ +
- ξ increases with vibrational energy, $v^+ = 0 - 4$. Consistent with $\mu_\Sigma(r_{BH}) - \mu_\Pi(r_{BH})$ inferred from *v*-dependence of Σ–Π splittings at low *N*

Conclusions

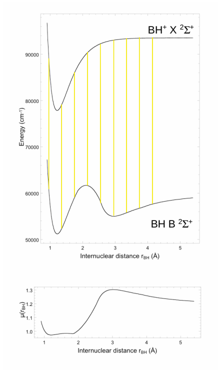

Distorted interatomic potentials confer Franck-Condon overlap on discrete-continuum and discrete-discrete transitions for which $\Delta v^{+} = \pm 1$ *(Fano lineshapes)*

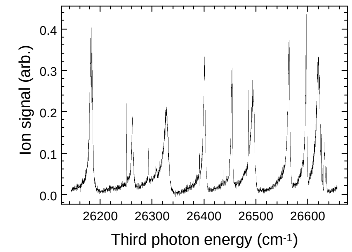

- Discrete structure supported on continua below and above vertical thresholds
- Vibrational overlap integrals for discrete-discrete and discrete-continuum transitions determine size of q and phase of interference
- r_{BH} - dependence of eigenchannel quantum defect tracks Franck-Condon factors, moderates effect on q, broadens resonances for higher v^{+}

Conclusions

Rydberg series below threshold appear in the $^{11}B^+$ mass channel following photoionization of $^{11}B^*$ dissociation products

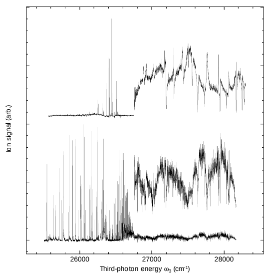

$^{11}BH^+$ signal is produced below threshold by core excitation on resonance for spectator Rydberg electrons. 10 ns laser absorption competes with (slow) dissociative loss.

Linewidths below threshold for (slow, $v^+ = 0$) predissociation compare with $v^+ = 1$ vibrational autoioniztion.

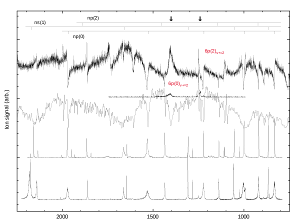

Above threshold, neutral dissociation competes with direct ionization (dissociative recombination).

Excitation along the B-H internuclear axis, along which dissociation occurs, favors electron loss.

Inelastic electron-cation scattering pathways leading to electron ejection and dissociative recombination proceed through a common continuum

On the production of a molecular Rydberg gas and its transformation to a cold plasma

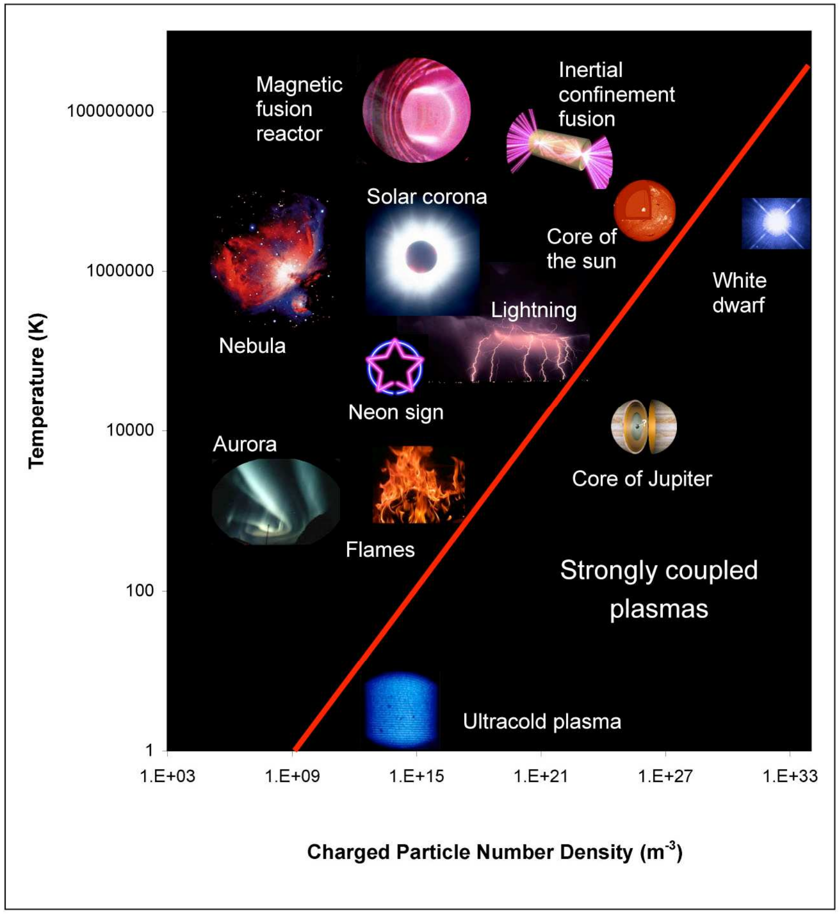

Plasmas in familiar energetic processes

Hot: Thermal E >> Coulomb E

Γ << 1 (no correlation)

Extreme cases, Γ > 1, liquid/solid like

$$\Gamma = \frac{q^2}{4\pi\varepsilon_0 a} \Big/ kT \qquad \frac{4}{3}\pi a^3 = \frac{1}{\rho}$$

Achieve at low density for low T

Integrate atomic & mesoscopic domains

Mott transition

Entanglement, quantum computing

As yet, no molecular examples

Back and forth between Rydberg atoms and ultracold plasmas

Gallagher et al. Vol. 20, No. 5 / May 2003 / J. Opt. Soc. Am. B 1091

Typically 10^{10} atoms cm^{-3} in a MOT at 100 μK

Excited by a few 100 μJ to principal quantum number n = 70

Evolves to plasma on the ns to μs time scale, $\Gamma \sim 1$

Disorder induced heating, T rises to a few K

Evaporative, expansion cooling

For molecules: Trapping/cooling are difficult

Cool to temperatures as low as 1 K, or lower in the moving frame of a supersonic expansion

Molecules cooled in a skimmed, seeded supersonic expansion

Density as high as 10^{15} molecules cm^{-3} T = 1K or less

Excited by as much as 10 mJ to principal quantum number n = 50, 60, 70, selected by double resonance

By analogy to atoms, evolution to plasma on the ns time scale.
Correlation?

For $\rho = 10^{12}\ cm^{-3}$

$$a^3 = \frac{3}{4\pi\left(10^{12} cm^{-3}\right)}; \quad a = 60\,\mu m$$

At T = 1 K, Γ = 0.28

But for molecular cations and electrons, question of dissociative recombination. Can plasma survive?

Experimental Apparatus

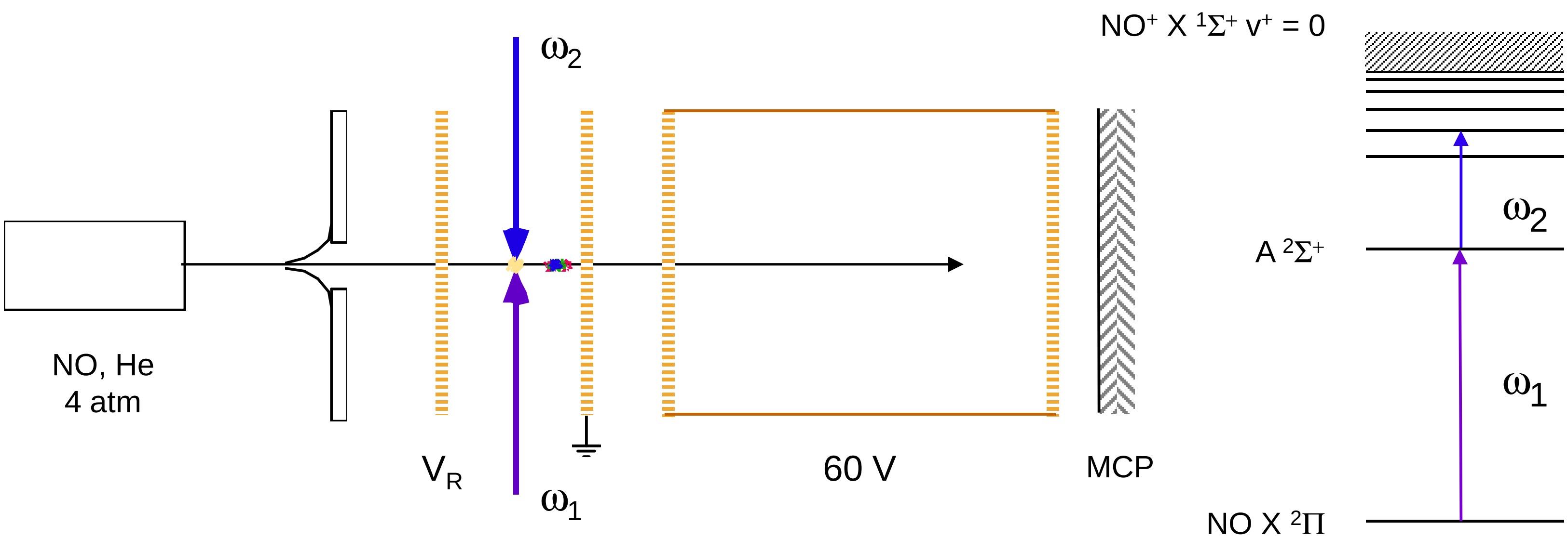

NSERC
CRSNG

Jonathan Morrison, Christopher Rennick,
Jamie Keller (Kenyon College)

Two-color selection of *52 f (2)*

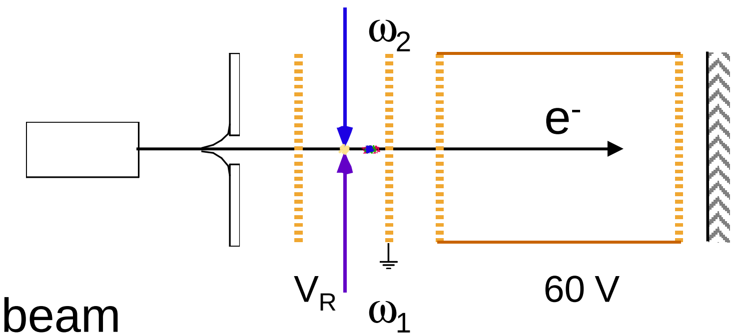

Late signal appears at the TOF of the molecular beam

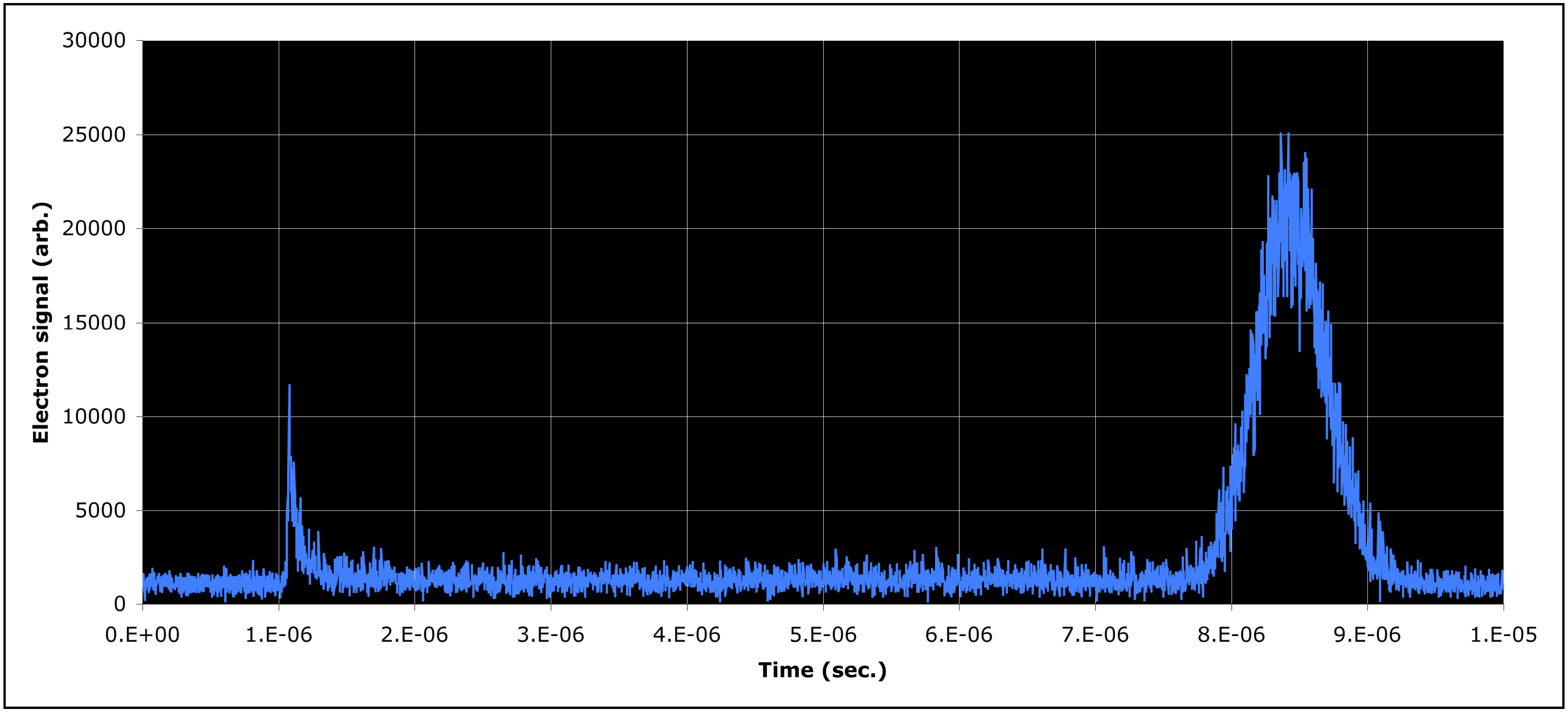

Contour plot showing the appearance time of the late signal as a function of principal quantum number

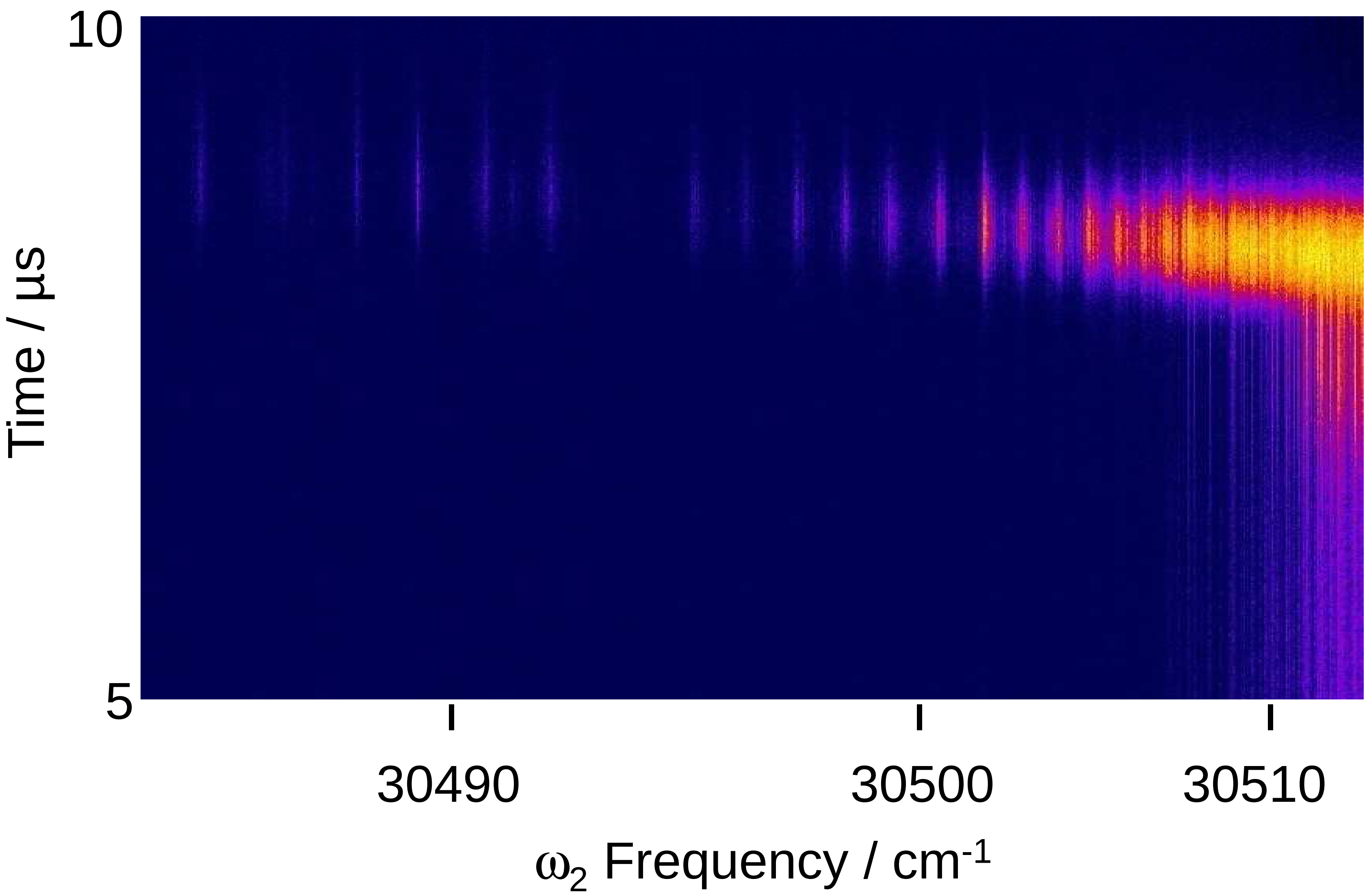

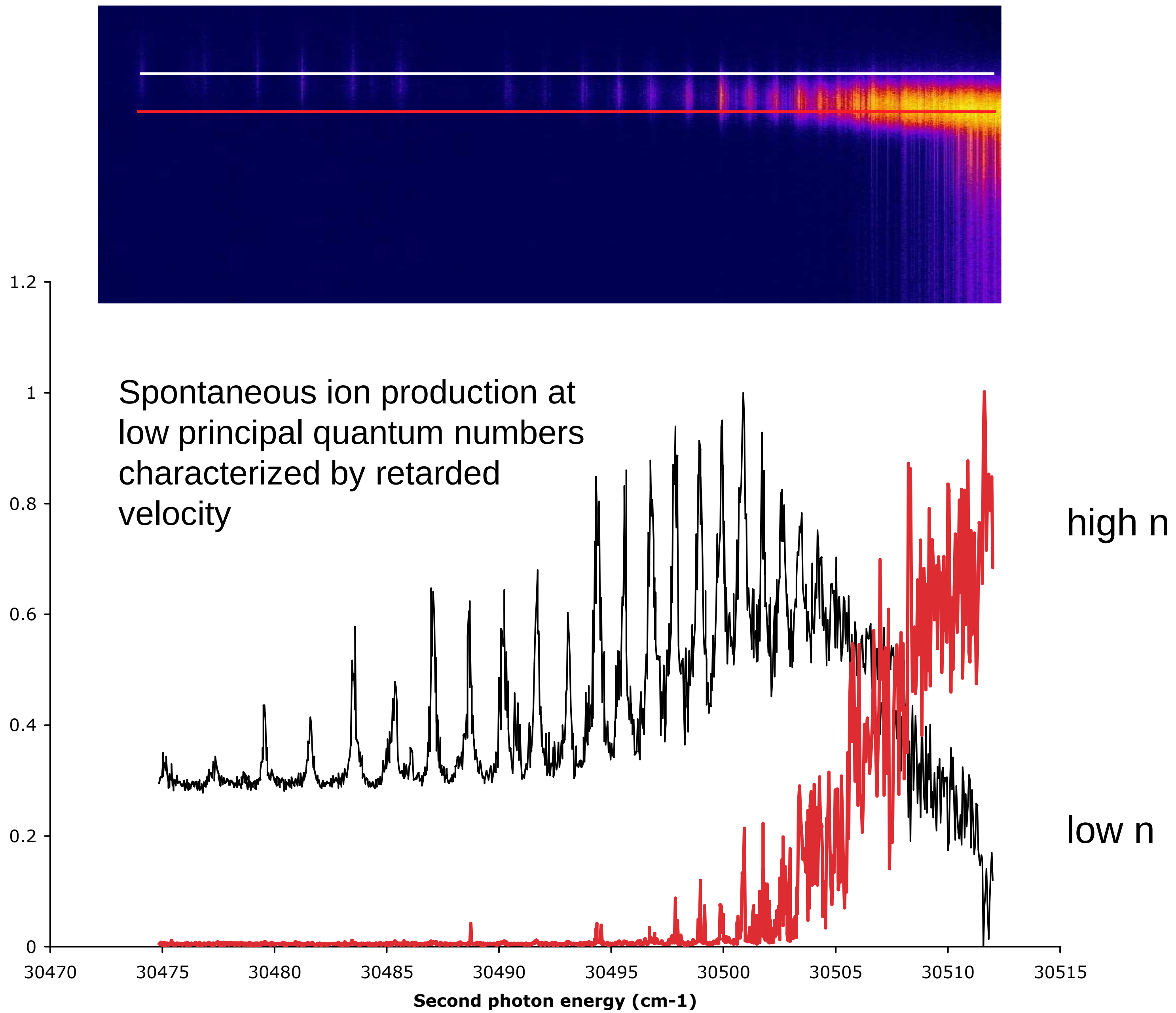

Spontaneous ion production at
low principal quantum numbers
characterized by retarded
velocity
high n
low n
1.2
1
0.8
0.6
0.4
0.2
0
30470
30475
30480
30485
30490
30495
30500
30505
30510
30515
Second photon energy (cm-1)

Velocity distributions measured by the passage of the charged ensemble through the extraction grid

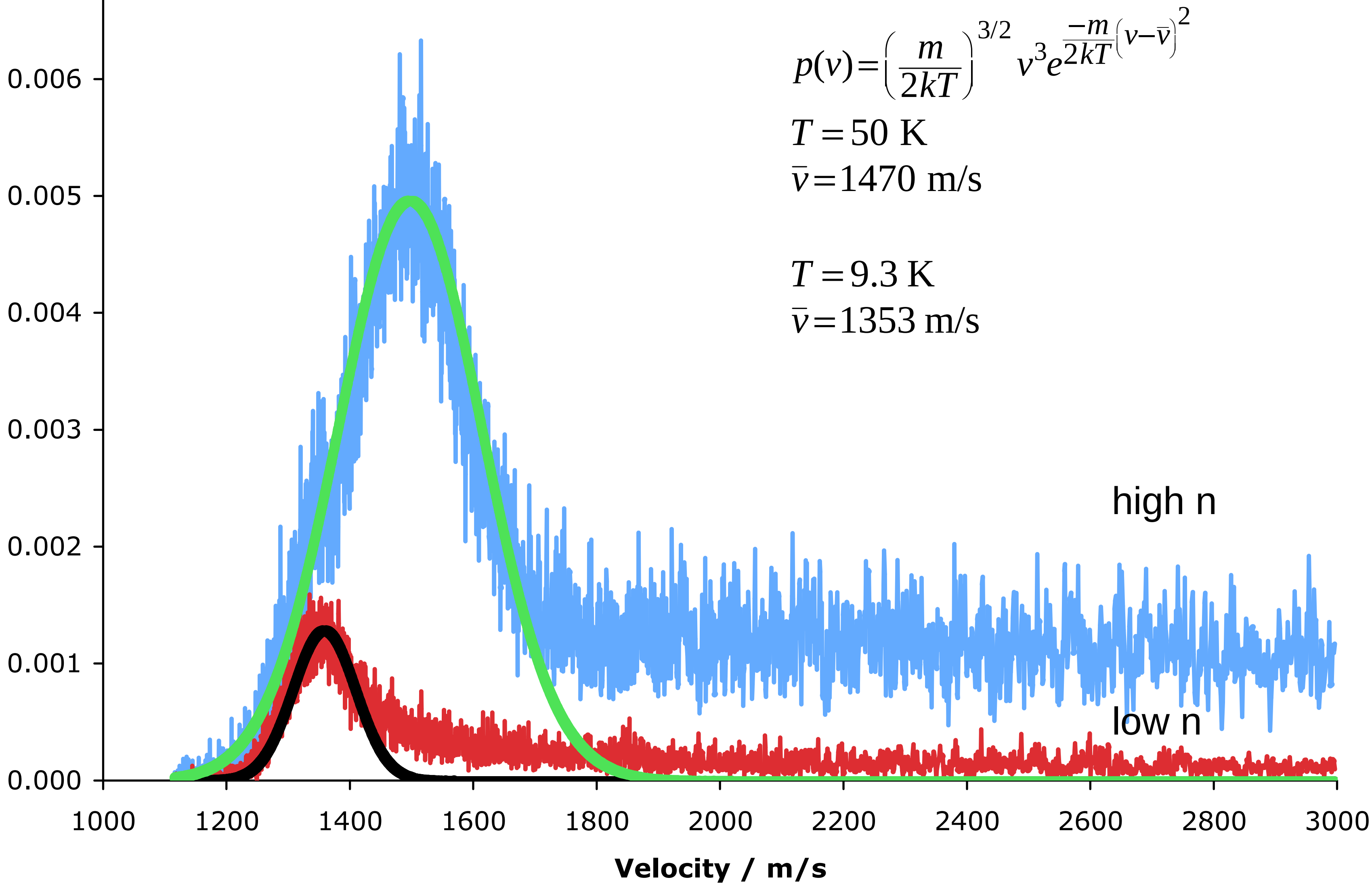

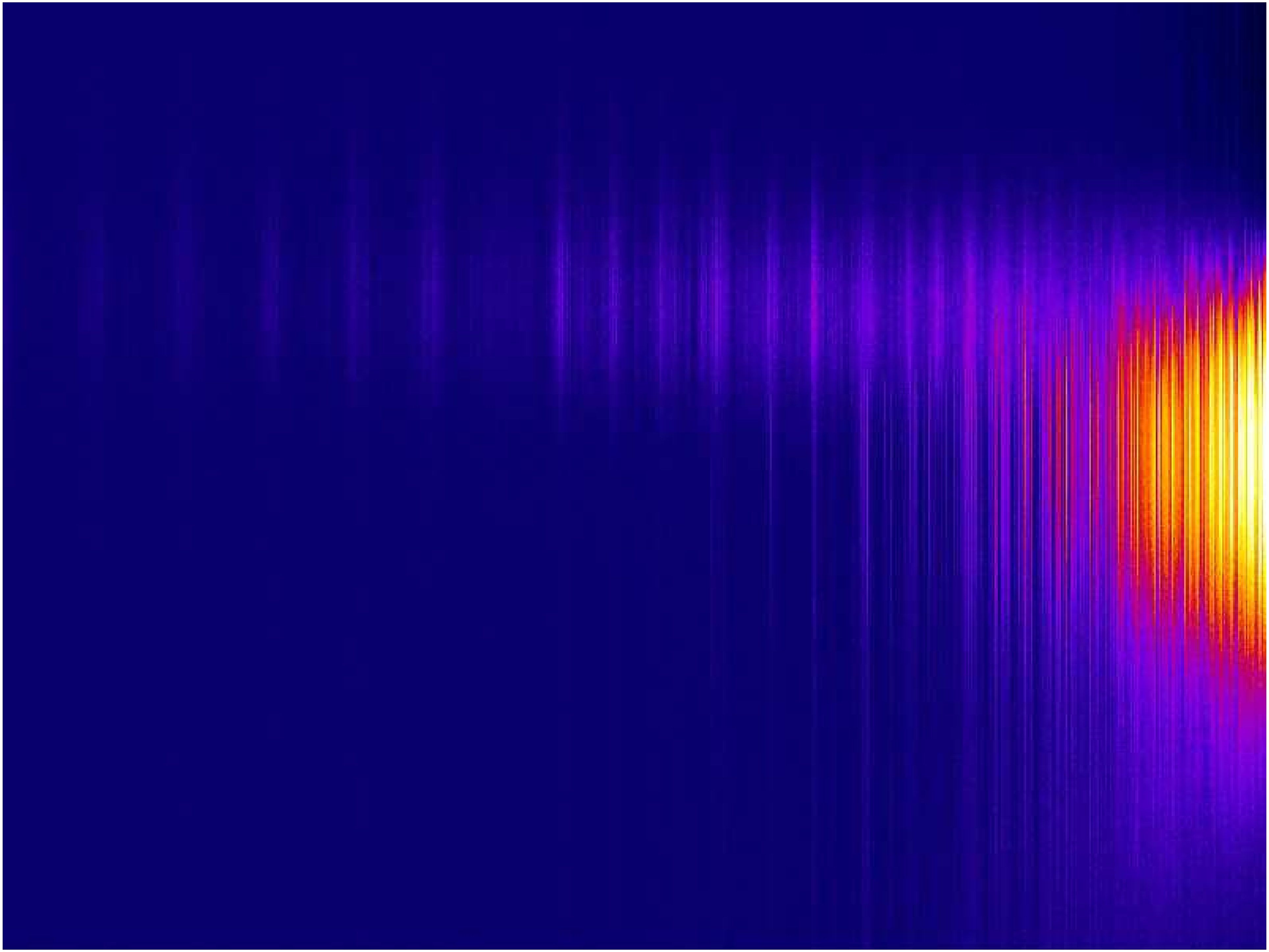

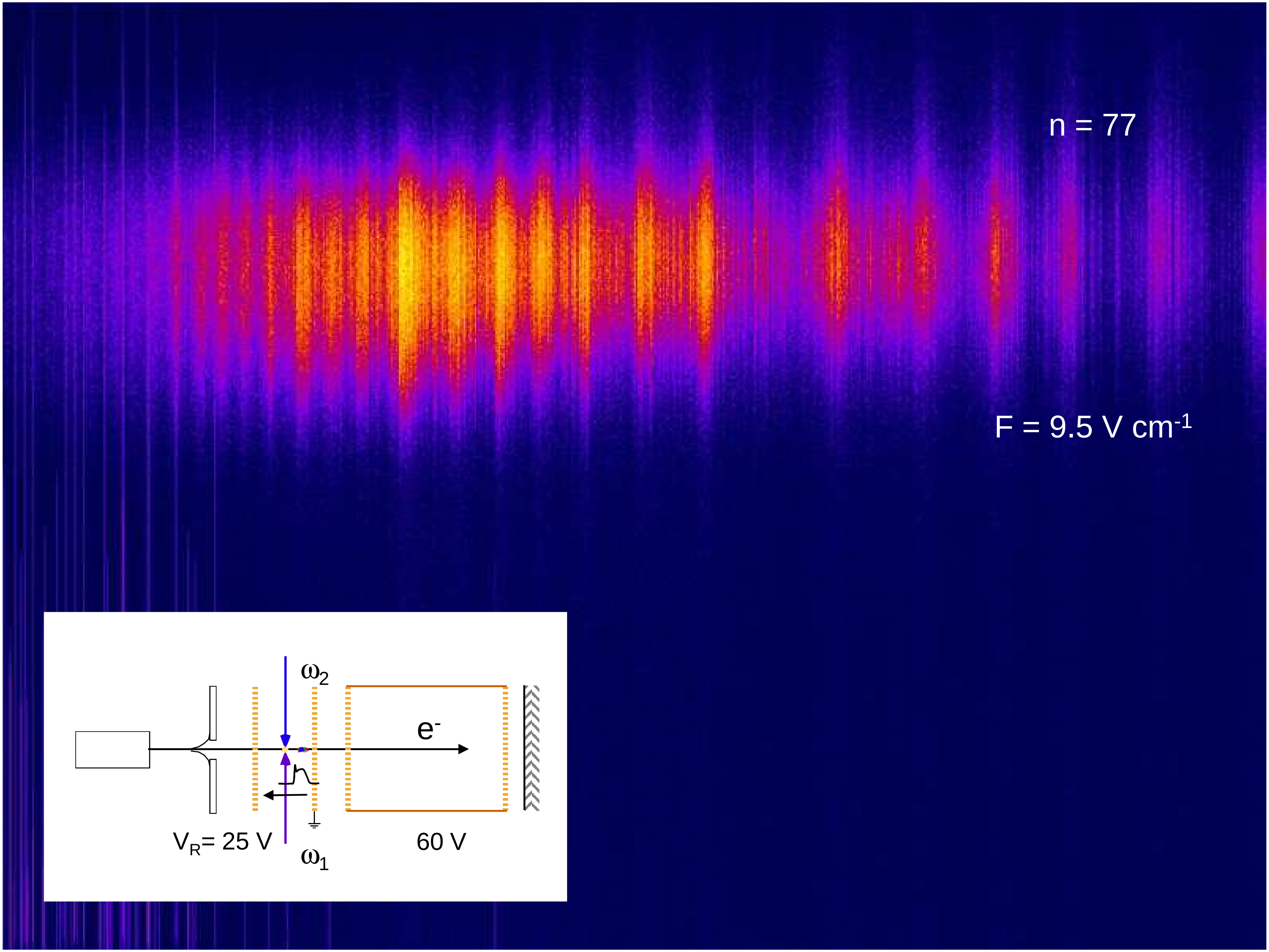
n = 77
F = 9.5 V cm^{-1}
ω_2
e$^-$
V_R= 25 V
60 V
ω_1

High-Rydberg resonances persist through delayed (1.5 µs) reverse bias PFI…

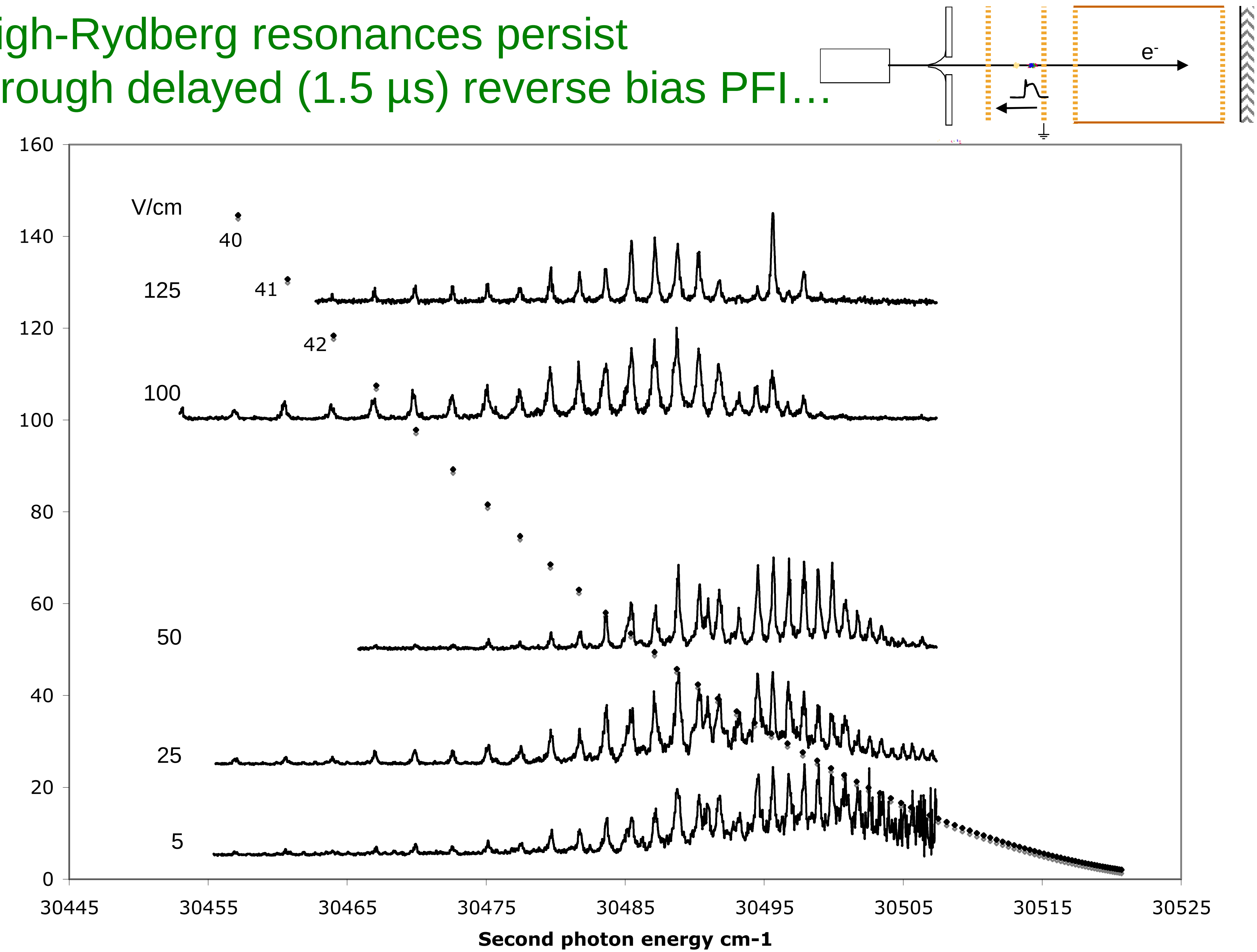

… but, the application of an electrostatic field at t = 0 suppresses late signal

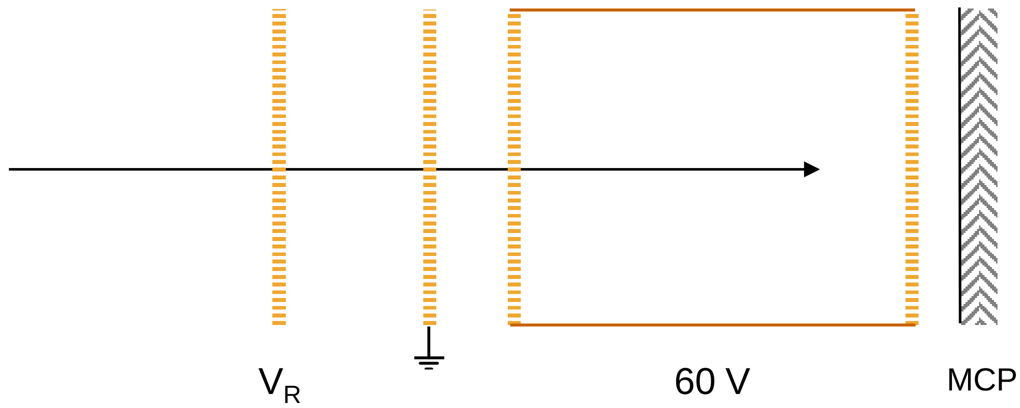

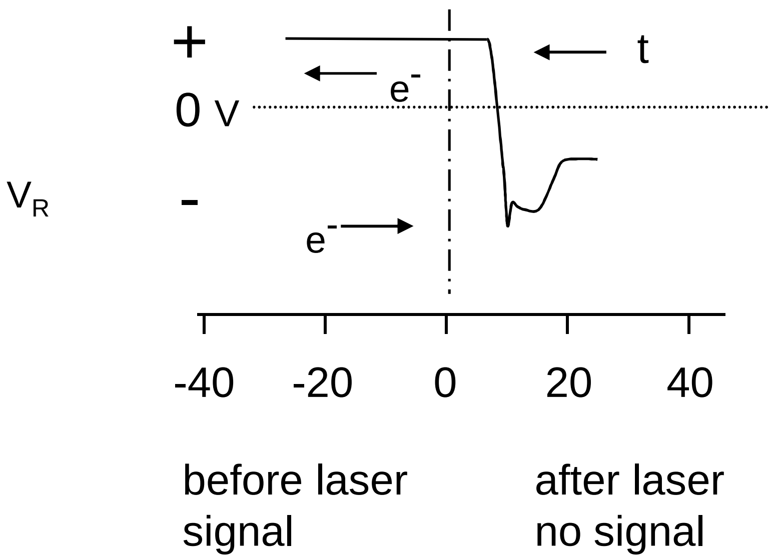

Monitor prompt electrons

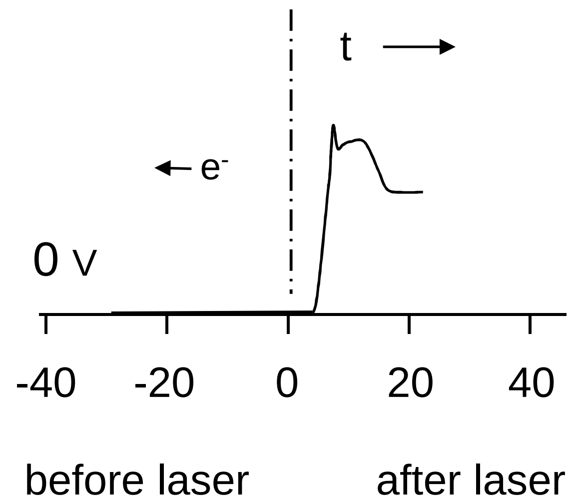

Monitor late (plasma) signal

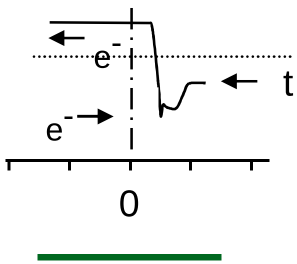

Effect of pulsed field on late signal when applied near t = 0

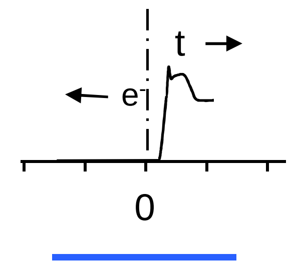

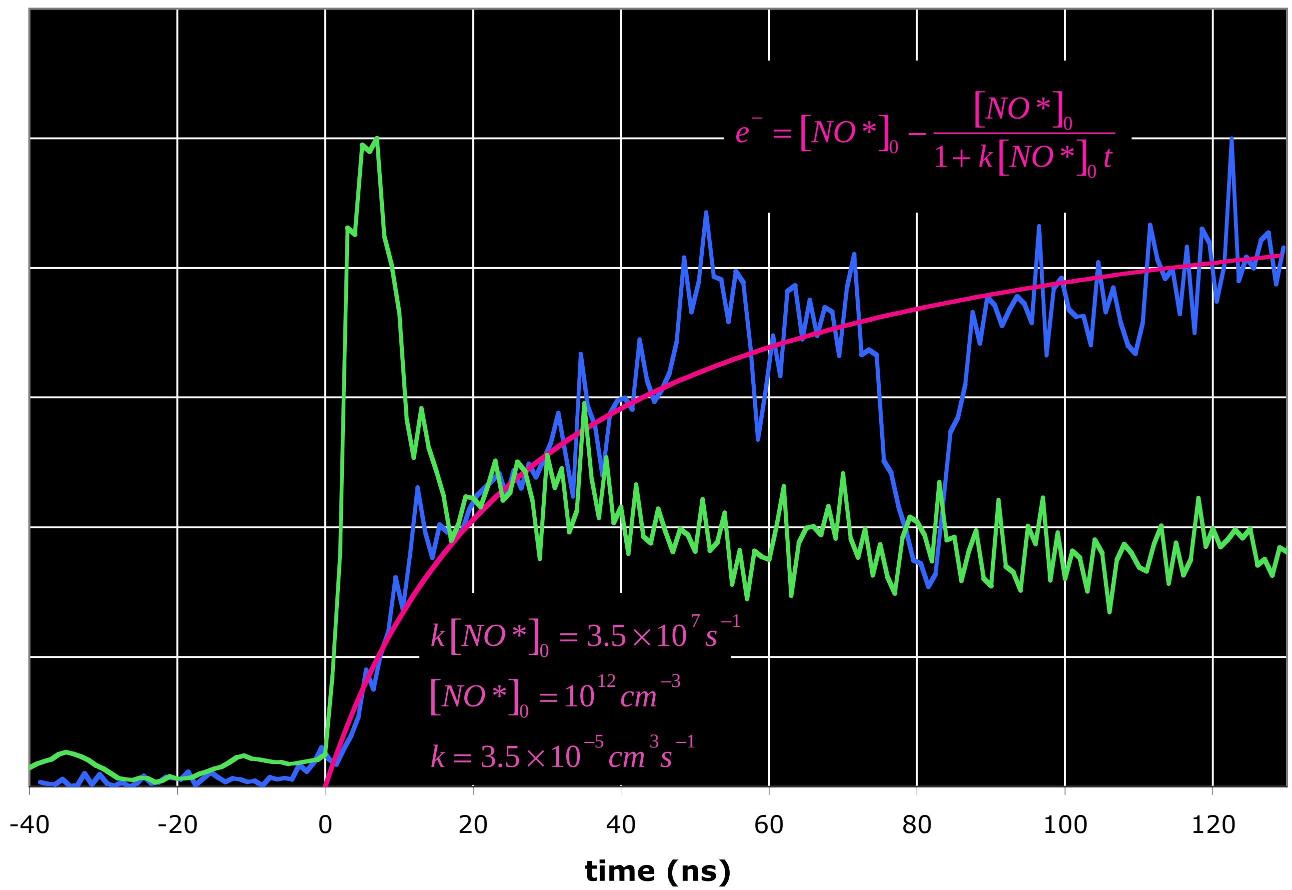

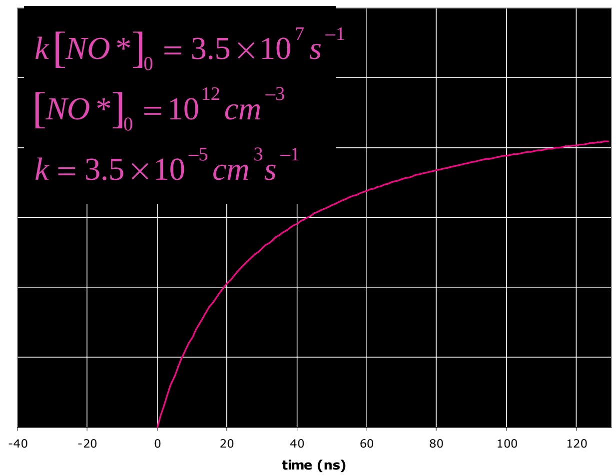

Is this a reasonable ionization rate?

Collision Theory

$$k = Z_{AA} e^{-E_a/k_B T}$$

$$Z_{AA} = \sigma_{AA}\sqrt{\frac{8\pi k_B T}{\mu}}$$

let $\sigma_{AA} = \pi\left(n^2 2a_0\right)^2$; for $n = 52$, $\sigma_{AA} = 2.6\times10^{-13} m^2$

for $T = 9$ K, $Z_{AA} = 9.2\times10^{-5} cm^3 s^{-1}$

Conclusions

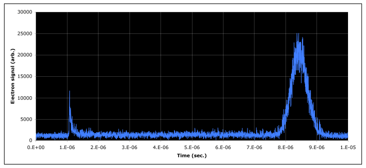

With sufficient excitation density, high-Rydberg states of NO form long-leved ensembles of charged particles.

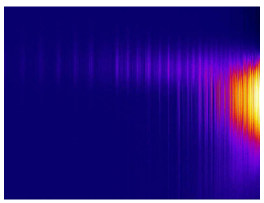

In warmer expansions, the process giving rise to this late signal favors the trailing ballistic fraction of the illuminated volume.

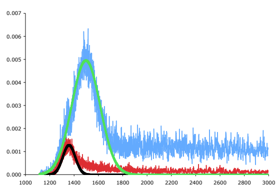

This portion of the distribution has a narrower velocity distribution (lower $T_{||}$ in the moving frame).

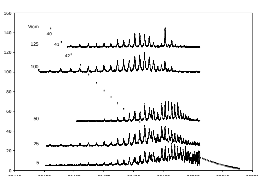

This late signal is resistant to reverse-bias, delayed pulsed-field ionization pluses of 125 V/cm and higher

Conclusions

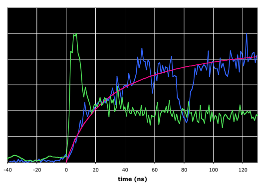

Application of an electrostatic field at t = 0 suppresses formation of the plasma.

Scanning the delay of this suppression field measures the time constant for plasma formation.

$$k[NO*]_0 = 3.5\times10^{7}\,s^{-1}$$
$$[NO*]_0 = 10^{12}\,cm^{-3}$$
$$k = 3.5\times10^{-5}\,cm^{3}s^{-1}$$

The rise-time observed in this way accords with the frequency of Rydber-Rydberg collisions at T ~ 9 K and $[NO^*]_0 = 10^{12}$ cm^{-1}.